

ON THE KERNEL OF THE SURGERY MAP RESTRICTED TO THE 1-LOOP PART

YUTA NOZAKI, MASATOSHI SATO, AND MASAAMI SUZUKI

ABSTRACT. Every homology cylinder is obtained from Jacobi diagrams by clasper surgery. The surgery map $\mathfrak{s}: \mathcal{A}_n^c \rightarrow Y_n \mathcal{IC}_{g,1} / Y_{n+1}$ is surjective for $n \geq 2$, and its kernel is closely related to the symmetry of Jacobi diagrams. We determine the kernel of \mathfrak{s} restricted to the 1-loop part after taking a certain quotient of the target. Also, we introduce refined versions of the AS and STU relations among claspers and study the abelian group $Y_n \mathcal{IC}_{g,1} / Y_{n+2}$ for $n \geq 2$.

CONTENTS

1. Introduction	1
2. Preliminaries	5
3. Refined surgery map and refined relations	7
4. Structures of modules of Jacobi diagrams	20
5. Kernel of \mathfrak{s} restricted to $\mathcal{A}_{n,1}^c$	26
6. Kernel of \mathfrak{s} restricted to $\mathcal{A}_{n,l}^c$ for $l > 1$	29
Appendix A. Alternative proof of Proposition 6.8	33
References	35

1. INTRODUCTION

Let $\Sigma_{g,1}$ be a compact oriented surface of genus g with one boundary component. In the study of the mapping class group $\mathcal{M}_{g,1}$ of $\Sigma_{g,1}$, the Torelli group $\mathcal{I} = \mathcal{I}_{g,1}$ is one of central interest. Here $\mathcal{I} = \mathcal{I}_{g,1}$ is defined to be the kernel of the natural homomorphism $\mathcal{M}_{g,1} \rightarrow \text{Aut } H_1(\Sigma_{g,1}; \mathbb{Z})$. One way to investigate $\mathcal{I} = \mathcal{I}_{g,1}$ is by considering its lower central series $\{\mathcal{I}(n)\}_{n \geq 1}$ defined by $\mathcal{I}(1) = \mathcal{I}$ and $\mathcal{I}(n+1) = [\mathcal{I}(n), \mathcal{I}]$ inductively. Goussarov [7] and Habiro [8] initiated the study of the monoid $\mathcal{IC} = \mathcal{IC}_{g,1}$ of homology cylinders over $\Sigma_{g,1}$, which can be regarded as a 3-dimensional analogue of \mathcal{I} . Here a homology cylinder is roughly a 3-manifold that is homologically the product of $\Sigma_{g,1}$ and the closed interval $[-1, 1]$. In their papers, clasper

2020 *Mathematics Subject Classification*. Primary 57K16, 57K31, Secondary 57K20.

Key words and phrases. Homology cylinder, Jacobi diagram, surgery map, clasper, LMO functor.

calculus in 3-manifolds was introduced. A clasper is a certain surface embedded in a 3-manifold, and one obtains another 3-manifold by surgery along the clasper. Using claspers, they introduced the Y_n -equivalence among 3-manifolds for any positive integer n and the Y -filtration $\{Y_n\mathcal{IC}\}_{n \geq 1}$ on \mathcal{IC} corresponding to $\{\mathcal{I}(n)\}_{n \geq 1}$. More precisely, we have an injective monoid homomorphism $\mathcal{I} \hookrightarrow \mathcal{IC}$ which maps $\mathcal{I}(n)$ into $Y_n\mathcal{IC}$. Furthermore, the map induces a homomorphism $\bigoplus_{n \geq 1} \mathcal{I}(n)/\mathcal{I}(n+1) \rightarrow \bigoplus_{n \geq 1} Y_n\mathcal{IC}/Y_{n+1}$ between abelian groups. Thus, determining $Y_n\mathcal{IC}/Y_{n+1}$ is significant to understand $\mathcal{I}(n)/\mathcal{I}(n+1)$ well. In fact, the authors [15] introduced an invariant $\bar{z}_{n+1}: Y_n\mathcal{IC}/Y_{n+1} \rightarrow \mathcal{A}_{n+1}^c \otimes \mathbb{Q}/\mathbb{Z}$ and extracted new information about $\mathcal{I}(n)/\mathcal{I}(n+1)$ which is not detected by the Johnson homomorphisms ([15, Theorem 1.2 and Corollary 1.4]). Furthermore, by combining [15, Theorem 1.2] with [14, Theorem 1.2], we conclude that the torsion subgroup $\text{tor}(\mathcal{I}(n)/\mathcal{I}(n+1))$ is non-trivial when $n = 3, 5$ and g is in a stable range. This is a generalization of the fact that $\text{tor}(\mathcal{I}(1)/\mathcal{I}(2)) \neq 0$. For more details of the groups $\mathcal{I}(n)/\mathcal{I}(n+1)$ and $Y_n\mathcal{IC}/Y_{n+1}$ we refer the reader to [15, Section 1].

Let \mathcal{A}_n^c denote the \mathbb{Z} -module generated by connected Jacobi diagrams with n trivalent vertices subject to the AS, IHX, and self-loop relations (to be defined later). Here a Jacobi diagram is a uni-trivalent graph with additional information. We can define the surgery map $\mathfrak{s}: \mathcal{A}_n^c \rightarrow Y_n\mathcal{IC}/Y_{n+1}$ by realizing a Jacobi diagram J as a clasper in the trivial homology cylinder $\Sigma_{g,1} \times [-1, 1]$, and \mathfrak{s} is surjective ([8, Section 8.5]) when $n \geq 2$. Hence, we focus on the kernel of \mathfrak{s} . Since $\mathfrak{s} \otimes \text{id}_{\mathbb{Q}}$ is known to be an isomorphism ([1, Theorem 7.11]), we conclude $\text{Ker } \mathfrak{s} \subset \text{tor } \mathcal{A}_n^c$. To investigate $\text{tor } \mathcal{A}_n^c$, we decompose \mathcal{A}_n^c into the direct sum $\bigoplus_{l \geq 0} \mathcal{A}_{n,l}^c$, where $\mathcal{A}_{n,l}^c$ denotes the submodule generated by Jacobi diagrams whose first Betti numbers are l . We write $\mathfrak{s}_{n,l}$ for the restriction of \mathfrak{s} to the l -loop part $\mathcal{A}_{n,l}^c$. The 0-loop part $\mathcal{A}_{n,0}^c$ was deeply studied by Conant, Schneiderman, and Teichner [3, 4, 5], and it was proved that $\text{tor } \mathcal{A}_{n,0}^c$ is generated by symmetric Jacobi diagrams of a particular form when n is odd. They applied their results to the study of the homology cobordism group $\mathcal{IH} = \mathcal{IH}_{g,1}$ of homology cylinders, which is the group obtained from \mathcal{IC} by identifying homology cylinders that are homology cobordant. In the study of \mathcal{IH} , one can ignore claspers having loops, namely the composite map $\mathcal{A}_{n,l}^c \xrightarrow{\mathfrak{s}_{n,l}} Y_n\mathcal{IC}/Y_{n+1} \twoheadrightarrow Y_n\mathcal{IH}/Y_{n+1}$ is trivial if $l \geq 1$ due to Levine [9], where $Y_n\mathcal{IH}$ denotes the image of $Y_n\mathcal{IC}$. On the other hand, $\mathfrak{s}_{n,l}$ itself is non-trivial in general, and it is hard to determine $\text{Ker } \mathfrak{s}_{n,l}$.

In this paper, we shall focus on the case $l = 1$ and determine $\text{Ker } \mathfrak{s}_{n,1}$ after taking a certain quotient of $Y_n\mathcal{IC}/Y_{n+1}$. First, we have to know the structure of the module $\text{tor } \mathcal{A}_{n,1}^c$, which was done in [15]. When n is odd, $\text{tor } \mathcal{A}_{n,1}^c$ is generated by symmetric 1-loop Jacobi diagrams illustrated in Figure 1, and we prove that certain pairs of such diagrams are in the kernel. To mention a rigorous statement, we introduce some modules and a quotient map. For

Theorem 1.2. *The abelian group $Y_3\mathcal{IC}/Y_5$ is torsion-free.*

Theorem 1.2 determines $Y_3\mathcal{IC}/Y_5$ (see also Remark 3.21). In particular, the above exact sequence does not split when $n = 3$. Furthermore, we can also apply our framework to the homology cobordism group \mathcal{IH} , and determine $Y_3\mathcal{IH}/Y_5$ in Theorem 3.22.



FIGURE 2. Process of blowing up a trivalent vertex.

Additionally, in Section 4, we investigate a useful relation between the 1-loop part $\mathcal{A}_{n,1}^c$ and the 2-loop part $\mathcal{A}_{n,2}^c$ to prove Theorem 1.1. Precisely, we focus on the map $\mathbf{bu}: \mathcal{A}_{n,l}^c \rightarrow \mathcal{A}_{n+2,l+1}^c$ defined by blowing up a trivalent vertex of a Jacobi diagram as in Figure 2.

Theorem 1.3. *The map \mathbf{bu} induces an isomorphism $\mathbf{bu}: \mathcal{A}_{n-2,1}^c \rightarrow \mathcal{A}_{n,2}^c / \langle \Theta_n^{\geq 1} \rangle$ for $n \geq 3$.*

As an application of Theorem 1.3, we solve the Goussarov-Habiro conjecture for the Y_5 -equivalence in Corollary 4.9. This conjecture asserts that the Y_n -equivalence among homology cylinders is characterized by finite type invariants of degree at most $n - 1$, which is one of the fundamental problems in quantum topology. The cases $n = 2, 3$ are known to be true (see [11, Section 2.3]), and the case $n = 4$ was solved in [15] as a consequence of the determination of the group $Y_3\mathcal{IC}/Y_4$.

Finally, we also discuss higher loop parts $\mathfrak{s}_{n,l}$ in Section 6. In contrast to the 1-loop part, we give lower bounds on the ranks of the $\mathbb{Z}/2\mathbb{Z}$ -modules $\text{Ker}(\mathfrak{s}|_{\text{tor } \mathcal{A}_{2k+1,k}^c})$ and $\text{Im}(\mathfrak{s}|_{\text{tor } \mathcal{A}_{2k+1,k}^c})$ for $k \geq 0$. See Theorem 6.9 for the precise statement. We use clasper calculus to study the kernel of $\mathfrak{s}_{2k+1,k}$. On the other hand, the image of $\mathfrak{s}_{2k+1,k}$ is investigated by the invariant \bar{z}_{2k+2} introduced in [15]. As a byproduct of the proof of Theorem 6.9, we conclude that the $(k + 1)$ -loop part $\bar{z}_{2k+2,k+1}$ of \bar{z}_{2k+2} is non-trivial in Corollary 6.7. Here we emphasize that its restriction to the torsion subgroup $\text{tor}(Y_{2k+1}\mathcal{IC}/Y_{2k+2})$ is still non-trivial and does not factor through the $(2k + 1)$ -st Johnson homomorphism. Note that $\bar{z}_{2k,0}$ and $\bar{z}_{2k,1}$ are already known to be non-trivial ([15, Corollary 1.4]).

Acknowledgments. This study was supported in part by JSPS KAKENHI Grant Numbers JP20K14317, JP20H05795, JP18K03310, JP20K03596, and JP19H01785.

2. PRELIMINARIES

We review homology cylinders, Jacobi diagrams, and the invariant \bar{z}_{n+1} of homology cylinders.

2.1. Homology cylinders. Let M be a connected oriented compact 3-manifold, and let $m: \partial(\Sigma_{g,1} \times [-1, 1]) \rightarrow \partial M$ be an orientation-preserving homeomorphism. Two pairs (M, m) and (M', m') are said to be equivalent if there is an orientation-preserving homeomorphism $f: M \rightarrow M'$ satisfying $f \circ m = m'$. Let m_{\pm} denotes the restriction of m to $\Sigma_{g,1} \times \{\pm 1\}$. A *homology cylinder* over $\Sigma_{g,1}$ is an equivalence class of a pair (M, m) such that m_+ and m_- induce the same isomorphism $H_*(\Sigma_{g,1}; \mathbb{Z}) \rightarrow H_*(M; \mathbb{Z})$. We define the composition of $M = (M, m)$ and $N = (N, n)$ by stacking N on M , that is, $M \circ N = (M \cup_{m_+ = n_-} N, m_- \cup n_+)$. Then the set $\mathcal{IC} = \mathcal{IC}_{g,1}$ of homology cylinders over $\Sigma_{g,1}$ is a monoid.

In the study of the monoid \mathcal{IC} , Goussarov [7] and Habiro [8] introduced claspers. Roughly speaking, a clasper in a 3-manifold is an embedded surface consisting of disks, bands, and annuli. Claspers allow us to introduce the Y_n -equivalence among homology cylinders and the submonoid $Y_n \mathcal{IC}$ of \mathcal{IC} . Also, the descending series $\mathcal{IC} = Y_1 \mathcal{IC} \supset Y_2 \mathcal{IC} \supset \cdots$ is called the *Y-filtration*. For the definitions of these terminologies, we refer the reader to [8] or [15, Sections 2.3 and 2.4]. It is known that the quotient set $Y_n \mathcal{IC} / Y_k$ is a finitely generated abelian group if $k \leq 2n$.

We sometimes express a homology cylinder by a $2g$ -component oriented tangle such as Example 3.3. In fact, there is a bijection between \mathcal{IC} and the set of bottom-top tangles in a homology cube ([1, Theorem 2.10]). The components of a bottom-top tangle correspond to the set $\{1^+, \dots, g^+, 1^-, \dots, g^-\}$. Throughout this paper, we fix a symplectic basis $\{\alpha_1, \dots, \alpha_g, \beta_1, \dots, \beta_g\}$ of $H = H_1(\Sigma_{g,1}; \mathbb{Z})$, and identify H with the module $\mathbb{Z}\{1^{\pm}, \dots, g^{\pm}\}$ according to $\alpha_i \leftrightarrow i^-$ and $\beta_i \leftrightarrow i^+$.

2.2. Jacobi diagrams. A *Jacobi diagram* is a uni-trivalent graph such that each trivalent vertex has a cyclic order and each univalent vertex is labeled by an element of the set $\{1^+, \dots, g^+, 1^-, \dots, g^-\}$. We define the *internal degree* $i\text{-deg } J$ of a Jacobi diagram J to be the number of trivalent vertices of J . Let \mathcal{A}_n (resp. \mathcal{A}_n^c) denote the \mathbb{Z} -module generated by Jacobi diagrams (resp. connected Jacobi diagrams) of $i\text{-deg} = n$ subject to the AS, IHX, and self-loop relations:

$$\begin{array}{c} \text{Y-vertex} + \text{Y-vertex} = 0, \quad \text{Box} - \text{Box} + \text{Box} = 0, \quad \text{Circle} = 0, \end{array}$$

where the rest of the diagrams are the same in each relation. Note that the IHX relation implies the self-loop relation among connected Jacobi diagrams of $i\text{-deg} \geq 2$.

Finally note that the subscripts of the map $\mathfrak{s}_{n,l}$ and $\bar{z}_{n+1,k}$ are both based on information about Jacobi diagrams, that is, the subscript of the $\mathfrak{s}_{n,l}$ (resp. $\bar{z}_{n+1,k}$) is the same as its domain (resp. codomain).

3. REFINED SURGERY MAP AND REFINED RELATIONS

In this section, we give refinements of the surgery map and the AS and STU relations among claspers to introduce some relations in $Y_n\mathcal{IC}/Y_{n+2}$ for $n \geq 2$.

3.1. Refined surgery map. Recall that the surgery map $\mathfrak{s}: \mathcal{A}_n^c \rightarrow Y_n\mathcal{IC}/Y_{n+1}$ is a homomorphism defined in terms of clasper surgeries corresponding to Jacobi diagrams labeled by $\{1^\pm, \dots, g^\pm\}$ in the trivial homology cylinder. See [1, Theorem 8.8], [8, Section 8.5], and [6, Theorem 4.13] for details. Here, we lift the target of the surgery map $\mathfrak{s}: \mathcal{A}_n^c \rightarrow Y_n\mathcal{IC}/Y_{n+1}$ to $Y_n\mathcal{IC}/Y_{n+2}$ when $n \geq 2$ to obtain relations of $Y_n\mathcal{IC}/Y_{n+2}$.

The ordinary surgery map \mathfrak{s} is defined as follows. For a connected Jacobi diagram J labeled by $\{1^\pm, 2^\pm, \dots, g^\pm\}$, we assign disks and annuli called nodes and leaves to trivalent and univalent vertices in J , respectively. By gluing them to bands corresponding to edges, we obtain a compact surface. To embed the surface into $\Sigma_{g,1} \times [-1, 1]$, fix an orientation of the surface, and identify $\Sigma_{g,1} \times [-1, 1]$ with the bottom-top tangle Id_g depicted in [1, Figure 2.6]. First, we embed each leaf along a meridian of a component of the tangle which represents the label of the corresponding univalent vertex. We assume that the annulus is vertical to the tangle, and that the orientation coincides with that of a fiber of the normal bundle of the tangle. Second, we embed the nodes in an arbitrary way, and also embed the bands in the complement of Id_g in $[-1, 1]^3$ so that the orientations of the constituents are compatible. In this way, we obtain a graph clasper in $\Sigma_{g,1} \times [-1, 1]$, and we denote its Y_{n+1} -equivalence class by $\mathfrak{s}(J)$. Here, we call a connected clasper without boxes a *graph clasper*.

To lift the target of the surgery map, we consider Jacobi diagrams with labels that have information on the relative positions of leaves with respect to the orientation of the tangle and of half-twists on edges.

Definition 3.1. Let J be a connected Jacobi diagram whose univalent vertices are labeled by the set

$$\mathcal{L} = \{1_j^\pm, \dots, g_j^\pm, \bar{1}_j^\pm, \dots, \bar{g}_j^\pm \mid j \in \mathbb{Z}_{\geq 1}\}$$

satisfying the condition that, for each $i^\epsilon \in \{1^\pm, \dots, g^\pm\}$, i_j^ϵ or \bar{i}_j^ϵ appears as a label in J exactly once for $j = 1, 2, \dots, n(i^\epsilon)$ for some $n(i^\epsilon) \geq 0$. Let us denote by $\tilde{\mathcal{J}}_n^c$ the set of such connected Jacobi diagrams J with $\text{i-deg}(J) = n$. As in the ordinary surgery map, in the label i_j^ϵ or \bar{i}_j^ϵ for $1 \leq i \leq g$ and $\epsilon = \pm$, the symbol i^ϵ corresponds to a component of the bottom-top tangle Id_g in the cube. The subscript j of i_j^ϵ or \bar{i}_j^ϵ indicates the relative position of a leaf among the leaves with respect to the orientation of the component

corresponding to the label i^ϵ , and the difference between the symbols i_j^ϵ and \bar{i}_j^ϵ is related to a positive half-twist on the edge incident to a leaf when realizing as a graph clasper.

Remark 3.2. In [8], a module $\mathcal{A}_n(\Sigma_{g,1})$ of Jacobi diagrams is defined, which is isomorphic to \mathcal{A}_n^c . Habiro used a total order on univalent vertices to denote the relative positions of leaves of a graph clasper. Instead, we adopt subscripts of labels to denote the relative positions of leaves.

We define the *refined surgery map*

$$\tilde{\mathfrak{s}}: \mathbb{Z}\tilde{\mathcal{J}}_n^c \rightarrow Y_n\mathcal{IC}/Y_{n+2}$$

in a similar way as the ordinary surgery map by embedding the compact oriented surface S corresponding to a connected Jacobi diagram. The first difference is that we choose some standard homotopy classes of edges when we embed S into the complement of the bottom-top tangle Id_g in $[-1, 1]^3$ as follows. First, we embed the $n(i^+)$ (resp. $n(i^-)$) copies of annuli corresponding to the univalent vertices labeled by i_j^+ and \bar{i}_j^+ (resp. i_j^- and \bar{i}_j^-) in a small neighborhood of the terminal point of the component i^+ (resp. the initial point of the component i^-) of the tangle for each $i = 1, 2, \dots, g$. We assume that the positions of leaves are arranged in order of the subscripts of the labels with respect to the orientation of the tangle. Second, we set disks as nodes in the subspace $\text{Int}([-1, 1] \times [-1, -1 + \delta] \times [-1, 1])$ of the cube, where $\delta > 0$ is sufficiently small. Corresponding to each edge in the Jacobi diagram incident to two trivalent vertices, we connect two nodes by a band in $\text{Int}([-1, 1] \times [-1, -1 + \delta] \times [-1, 1])$ so that the orientations are compatible. Lastly, to embed the rest of the edges, we draw a line which is parallel to the second coordinate axis from each leaf to the plane $[-1, 1] \times \{-1 + \delta\} \times [-1, 1]$, and we connect the end points of lines in the plane to the corresponding nodes by arcs in $(-1, 1) \times (-1, -1 + \delta] \times (-1, 1)$. By fattening the lines and arcs to bands so that the orientations are compatible with the nodes and leaves, we obtain embedded edges.

The second difference is that, if the label of a univalent vertex is of the form \bar{i}_j^ϵ , we apply a positive half-twist when we connect the band to the corresponding leaf.

For elements a_1, a_2, \dots, a_n in \mathcal{L} satisfying the condition in Definition 3.1 (resp. in $\{1^\pm, 2^\pm, \dots, g^\pm\}$), let us denote

$$T(a_1, a_2, \dots, a_n) = \begin{array}{ccccccc} & & a_2 & a_3 & & a_{n-1} & \\ & & \vdots & \vdots & \cdots & \vdots & \\ a_1 & \cdots & \cdots & \cdots & \cdots & \cdots & a_n \end{array}$$

which is an element in $\mathbb{Z}\tilde{\mathcal{J}}_{n-2}^c$ (resp. in \mathcal{A}_{n-2}^c).

Example 3.3. The image of $T(1_1^-, 1_2^+, 1_1^+, \bar{2}_1^-) \in \mathbb{Z}\tilde{\mathcal{J}}_2^c$ under the refined surgery map $\tilde{\mathfrak{s}}: \mathbb{Z}\tilde{\mathcal{J}}_2^c \rightarrow Y_2\mathcal{IC}_{2,1}/Y_4$ is

$$\tilde{\mathfrak{s}}(T(1_1^-, 1_2^+, 1_1^+, \bar{2}_1^-)) = \begin{array}{c} \begin{array}{c} \text{Diagram of a graph clasper with four vertical strands and various crossings and half-twists.} \end{array} \\ \in Y_2\mathcal{IC}_{2,1}/Y_4, \end{array}$$

where \oplus in the figure denotes a positive half-twist.

Lemma 3.4. For $n \geq 2$, the refined surgery map $\tilde{\mathfrak{s}}: \mathbb{Z}\tilde{\mathcal{J}}_n^c \rightarrow Y_n\mathcal{IC}/Y_{n+2}$ is a well-defined homomorphism.

Proof. Before discussing $\tilde{\mathfrak{s}}$, we recall that there are three ambiguities when we embed the surface corresponding to a connected Jacobi diagram labeled by $\{1^\pm, \dots, g^\pm\}$ in the definition of \mathfrak{s} ; framings of edges, isotopy classes of edges, and positions of leaves, where the third ambiguity occurs only when multiple vertices have the same label. Recall that the ordinary surgery map $\mathfrak{s}: \mathcal{A}_n^c \rightarrow Y_n\mathcal{IC}/Y_{n+1}$ is well-defined because the first ambiguity is eliminated by edge twists ([16, Lemma E.7]), the second one is eliminated by edge slidings ([16, Lemma E.5], [11, Lemma A.1]), and the third one is also eliminated by leaf crossings ([16, Lemma E.6]). If we try to lift the target of the surgery map from the Y_{n+1} -equivalence classes to the Y_{n+2} -equivalence classes, full-twists along edges are still eliminated using [11, Lemmas A.1 and A.5] with respect to a connected sum of an edge with a trivial knot with (-1) -framing. With respect to the second ambiguity, we cannot slide an edge of a graph clasper as in [11, Lemma A.1], although we can still apply a crossing change of edges in a graph clasper up to Y_{n+2} -equivalence in the same way as [8, Proposition 4.6]. The proof is almost the same except that the subtree T in the proof of [8, Proposition 4.6] is of degree $n+2$ (in our notation) after the zip construction. Thus, we need to fix the homotopy classes of edges as we did in the refined surgery map. Because of the third ambiguity, we assigned the subscript j in the labels of J , and the positions of the leaves attaching to the same component of the tangle are ordered.

By edge slidings ([12, Lemma 2.6(2)(a)]) and leaf crossings based on [12, Lemma 2.6(2)(b)] of two graph claspers, we can also show that $\tilde{\mathfrak{s}}$ is a homomorphism in the same way as \mathfrak{s} . \square

Remark 3.5. Full twists along edges of a graph clasper of degree n do not change its Y_{n+2} -equivalence class. Thus, it does not matter whether we apply a positive or negative half-twist to an edge in the refined surgery map $\tilde{\mathfrak{s}}$ when the label of a univalent vertex is of the form \bar{i}^ϵ .

Define a map

$$\varpi: \mathcal{L} \rightarrow \{1^\pm, \dots, g^\pm\},$$

by $i_j^\pm \mapsto i^\pm$ and $\bar{i}_j^\pm \mapsto i^\pm$. We also define a homomorphism

$$\mathcal{P}: \mathbb{Z}\tilde{\mathcal{J}}_n^c \rightarrow \mathcal{A}_n^c$$

by $\mathcal{P}(J) = (-1)^k \bar{J}$, where \bar{J} is the Jacobi diagram obtained by changing the labels of the univalent vertices in $J \in \mathbb{Z}\tilde{\mathcal{J}}_n^c$ by ϖ , and k is the number of univalent vertices in J colored by $\{\bar{1}_j^\pm, \dots, \bar{g}_j^\pm \mid j \in \mathbb{Z}_{\geq 1}\} \subset \mathcal{L}$. The AS relation in \mathcal{A}_n^c implies that if we apply a half-twist to an edge in a graph clasper representing $\mathfrak{s}(\bar{J})$, then the sign of its Y_{n+1} -equivalence class changes. Thus, we have a commutative diagram

$$\begin{array}{ccc} \mathbb{Z}\tilde{\mathcal{J}}_n^c & \xrightarrow{\tilde{\mathfrak{s}}} & Y_n\mathcal{IC}/Y_{n+2} \\ \mathcal{P} \downarrow & & \downarrow \\ \mathcal{A}_n^c & \xrightarrow{\mathfrak{s}} & Y_n\mathcal{IC}/Y_{n+1} \end{array}$$

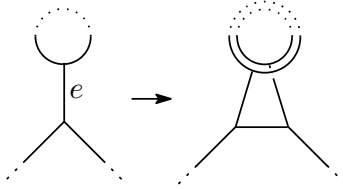
for $n \geq 2$, where the right vertical map is the natural projection.

3.2. Refined AS and refined STU relations. Here, we introduce the refined AS and refined STU relations, and introduce some relations in $Y_n\mathcal{IC}/Y_{n+2}$.

Lemma 3.6. *Let $n \geq 1$, and let G be a graph clasper with n nodes in $\Sigma_{g,1} \times [-1, 1]$. We denote by G' the graph clasper obtained from G by inserting a positive half-twist in one edge e .*

If e is incident to a leaf and a node in G , denote by H the graph clasper obtained by doubling a neighborhood of e as below. Then, we have

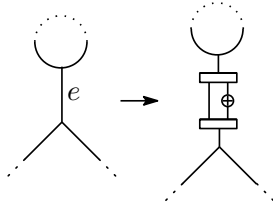
$$(\Sigma_{g,1} \times [-1, 1])_G \circ (\Sigma_{g,1} \times [-1, 1])_{G'} \circ (\Sigma_{g,1} \times [-1, 1])_H \sim_{Y_{n+2}} \Sigma_{g,1} \times [-1, 1].$$



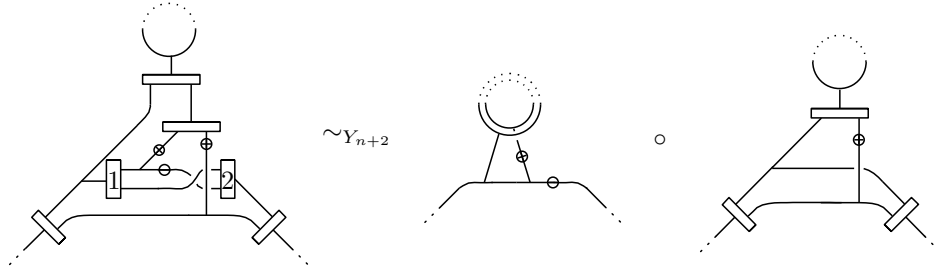
If e is incident to two nodes in G , we have

$$(\Sigma_{g,1} \times [-1, 1])_G \circ (\Sigma_{g,1} \times [-1, 1])_{G'} \sim_{Y_{n+2}} \Sigma_{g,1} \times [-1, 1].$$

Proof. Assume that e is incident to a leaf and a node. In [11, Lemma A.9], the case $n = 1$ is treated. The proof is based on their clasper calculus. If we change a neighborhood of e in G as below, it is equivalent to the empty one by Move 4 in [8].

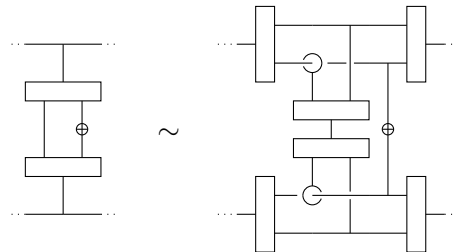


It is also equivalent to the left-hand side below as in the proof of [11, Lemma A.9], where \ominus denotes a negative half-twist.

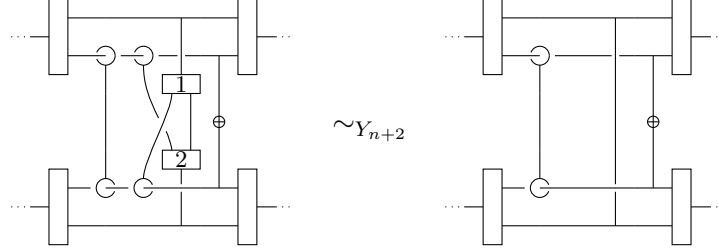


By the zip construction with the upper input of Box 1 and the lower input of Box 2 as a marking and by applying Move 5 in [8] several times, we obtain a graph clasper of degree $n + 1$, which is the first one on the right-hand side. By edge slidings ([12, Lemma 2.6(2)(a)]) and leaf crossings based on [12, Lemma 2.6(2)(b)], we can separate it from the rest up to Y_{n+2} -equivalence, and the corresponding homology cylinder decomposes into a product of two homology cylinders as in the right-hand side. By [16, Lemma E.7 or (E.10)], the first one is represented by $(\Sigma_{g,1} \times [-1, 1])_H$ up to Y_{n+2} -equivalence. In the second homology cylinder, apply the zip construction with the left input of the lower-left box and the right input of the lower-right box as a marking. Then, it decomposes into the product $(\Sigma_{g,1} \times [-1, 1])_G \circ (\Sigma_{g,1} \times [-1, 1])_{G'}$. Here, to erase extra boxes arising from the zip construction, we applied Move 12 to the leaf attached to an input of each extra box and the zip construction, and erased graph claspers of degree $n + 2$. We also used Move 11 on extra boxes to increase the degrees of the graph claspers. It is also possible to erase extra boxes by applying Move 11, crossing changes ([12, Lemma 2.6(2)(b)]) of edges and leaves, and Move 3. If the graph clasper G has loops, there arise pairs of boxes whose outputs are connected by one edge. We also used the move [8, Figure 38] and the zip construction to erase these boxes.

Next, we treat the case where e is incident to two nodes. In the same way, consider the clasper obtained by changing a neighborhood of e as on the left-hand side below.



Using Move 11 twice, we have the clasper on the right-hand side. By the move [8, Figure 38] and Move 6, it is equivalent to the clasper on the left-hand side below.



By the zip construction with the four edges incident to the twisted edge as a marking, we obtain a graph clasper of degree n as a subset of the resulting clasper. Thus, after applying Move 11 to Boxes 1 and 2 so that each of the two leaves attached to the left inputs is incident to a node, we can pass horizontal edges in the figure across the two leaves up to Y_{n+2} -equivalence by [12, Lemma 2.6(2)(b)]. Applying Move 3 to erase Boxes 1 and 2 and the same zip construction backward, we obtain the clasper on the right-hand side. The graph clasper with no node and two leaves in the figure corresponds to a crossing change of two edges, and we can also erase it up to Y_{n+2} -equivalence as we explained in the proof of Lemma 3.4. After applying the same zip construction, we can separate the graph clasper of degree n from the rest by edge slidings [12, Lemma 2.6(2)(a)] and leaf crossings [12, Lemma 2.6(2)(b)], and the homology cylinder decomposes into the product $(\Sigma_{g,1} \times [-1, 1])_G \circ (\Sigma_{g,1} \times [-1, 1])_{G'}$. \square

Let $J \in \tilde{\mathcal{J}}_n^c$ be a connected Jacobi diagram, and let v be one of its univalent vertices. Similar to the first term of $\delta_v(J)$ in Definition 2.1, we consider the Jacobi diagram J_v obtained by doubling a neighborhood of the edge incident to v , and change the labels of all the univalent vertices by the map ϖ . Let us denote by

$$\tilde{\delta}_v(J) = (-1)^k J_v \in \mathcal{A}_{n+1}^c,$$

where k is the number of univalent vertices in J , except v , labeled by $\{\bar{1}_j^\pm, \dots, \bar{g}_j^\pm \mid j \in \mathbb{Z}_{\geq 1}\}$. By the former half of Lemma 3.6, we obtain the following.

Corollary 3.7 (refined AS relation). *Let $n \geq 2$. For a connected Jacobi diagram $J \in \tilde{\mathcal{J}}_n^c$, we denote by J' the Jacobi diagram obtained by changing the label of one univalent vertex v in J as $\ell(v) \mapsto \overline{\ell(v)}$. Then, we have*

$$\tilde{\mathfrak{s}}(J) + \tilde{\mathfrak{s}}(J') + \mathfrak{s}(\tilde{\delta}_v(J)) = 0 \in Y_n \mathcal{IC} / Y_{n+2}.$$

Note that Corollary 3.7 implies the move in [16, Lemma E.9], which corresponds to the AS relation in \mathcal{A}_n^c . For $n \geq 2$, let us define a homomorphism

$$\text{rev}: \mathbb{Z} \tilde{\mathcal{J}}_n^c \rightarrow \mathbb{Z} \tilde{\mathcal{J}}_n^c$$

by the map which changes the cyclic order of every trivalent vertex to the other one, and changing the label $a \in \mathcal{L}$ of each univalent vertex into \bar{a} . Here, we regard $\bar{\bar{a}}$ as a . Note that we have

$$\tilde{\mathfrak{s}}(\text{rev}(J)) = \tilde{\mathfrak{s}}(J) \quad (3.1)$$

for $J \in \tilde{\mathcal{J}}_n^c$ because if we reverse neighborhoods of all the nodes of the graph clasper corresponding to $\tilde{\mathfrak{s}}(J)$, we obtain the graph clasper corresponding to $\tilde{\mathfrak{s}}(\text{rev}(J))$.

Using Corollary 3.7, we obtain relations in $Y_n\mathcal{IC}/Y_{n+2}$.

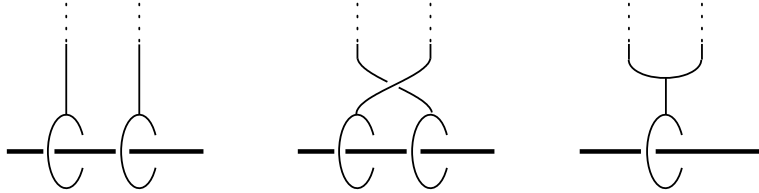
Example 3.8. Let $a_1, a_2, \dots, a_n \in \{1_1^\pm, \dots, g_1^\pm\} \subset \mathcal{L}$ be mutually distinct elements. We have

$$\begin{aligned} \tilde{\mathfrak{s}}(T(a_1, a_2, \dots, a_n)) &= \tilde{\mathfrak{s}}(\text{rev}(T(a_1, a_2, \dots, a_n))) \\ &= \tilde{\mathfrak{s}}(T(\bar{a}_n, \dots, \bar{a}_2, \bar{a}_1)) \\ &= (-1)^n \sum_{i=1}^n \tilde{\mathfrak{s}}(T(\varpi(a_n), \dots, \varpi(a_{i+1}), \varpi(a_i), \varpi(a_i), \varpi(a_{i-1}), \dots, \varpi(a_1))) \\ &\quad + (-1)^n \tilde{\mathfrak{s}}(T(a_n, \dots, a_2, a_1)). \end{aligned}$$

Next, we introduce the refined STU relation. The following lemma is well-known. See the proof of Proposition 4.4 and Figure 29(a)–(f) in [8]. See also [13, Lemma 2.2(1)].

Lemma 3.9. *Let $n \geq 1$, and let G be a graph clasper with n nodes in a 3-manifold M whose two leaves are locally described as in the left-hand side below, where the thick lines imply the same bundle which may contain edges and leaves of claspers. Let G' be the graph clasper obtained from G by swapping the positions of the two leaves as in the middle, and let H be the graph clasper obtained by merging two leaves into one leaf as in the right-hand side. Then, we have*

$$M_{G'} \sim_{Y_{n+2}} M_{G \cup H}.$$



Let $J \in \tilde{\mathcal{J}}_n^c$ be a connected Jacobi diagram, and let v and w be two univalent vertices of J with labels i_j^ϵ and i_{j+1}^ϵ for some $j = 1, 2, \dots, n(i^\epsilon) - 1$, respectively. Similar to $\delta_{vw}(J)$ in Definition 2.1, we consider the Jacobi diagram J_{vw} obtained by gluing a Y -shaped graph along the vertices v and w in J . We set the label of the other univalent vertex in the Y -shaped graph by i^ϵ and change the labels of the other univalent vertices in J_{vw} by the map

ϖ . Here, note that we choose the cyclic order of the trivalent vertex of the Y -shaped graph as in the figure of $\delta_{vw}(J)$. Let us denote by

$$\tilde{\delta}_{vw}(J) = (-1)^k J_{vw} \in \mathcal{A}_{n+1}^c,$$

where k is the number of univalent vertices in J labeled by $\{\bar{1}_j^\pm, \dots, \bar{g}_j^\pm \mid j \in \mathbb{Z}_{\geq 1}\}$. By Lemma 3.9, we obtain the following.

Corollary 3.10 (refined STU relation). *Let $n \geq 2$, and let $J \in \tilde{\mathcal{J}}_n^c$ be a connected Jacobi diagram with two vertices v and w labeled by i_j^ϵ and i_{j+1}^ϵ for some $j = 1, 2, \dots, n(i^\epsilon) - 1$, respectively. We denote by J' the Jacobi diagram obtained by exchanging the labels of v and w in J . Then, we have*

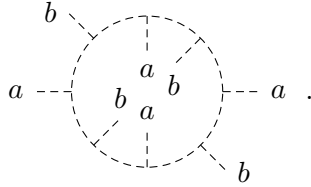
$$\tilde{\mathfrak{s}}(J') = \tilde{\mathfrak{s}}(J) + \mathfrak{s}(\tilde{\delta}_{vw}(J)) \in Y_n \mathcal{IC} / Y_{n+2}.$$

3.3. Applications of refined relations and symmetric and reversible Jacobi diagrams. Here, we give some relations among clasper surgeries along reversible and symmetric Jacobi diagrams defined below, and prove Theorem 1.2.

For a connected Jacobi diagram J labeled by $\{1^\pm, \dots, g^\pm\}$, let us denote by J' the Jacobi diagram obtained by reversing the cyclic order of every trivalent vertex to the other one. We call J *reversible* if J' is isomorphic to J as a Jacobi diagram, namely as a uni-trivalent graph endowed with cyclic orders on the trivalent vertices and labels on the univalent vertices. Note that, when $n = \text{i-deg } J$ is odd, we obtain $2J = 0 \in \mathcal{A}_n^c$ by the AS relation. Forgetting the cyclic orders, we can identify J' with J , and the above isomorphism $J' \rightarrow J$ gives an isomorphism $r: J \rightarrow J$ of uni-trivalent graphs, not of Jacobi diagrams. We call it a *reversing map* of J . Note that the Jacobi diagram $J = \theta(a, b; c, c; b, a)$ satisfies $J = J' \in \mathcal{A}_8^c$, but J is not reversible if $a \neq b$.

A connected Jacobi diagram J labeled by $\{1^\pm, \dots, g^\pm\}$ is called *symmetric* if it is symmetric along some line when depicted in a diagrammatic form in \mathbb{R}^2 . For example, the Jacobi diagrams $T(a_1, a_2, \dots, a_n, a_n, \dots, a_2, a_1)$ and $T(a_1, a_2, \dots, a_n, \dots, a_2, a_1)$ are symmetric for $n \geq 2$ with respect to the center lines when depicted as the one just before Example 3.3. Let $\mathcal{A}_n^{c,s}$ denote the submodule of \mathcal{A}_n^c generated by symmetric Jacobi diagrams, which decomposes as $\bigoplus_{l \geq 0} \mathcal{A}_{n,l}^{c,s}$.

Symmetric Jacobi diagrams are reversible, and the line symmetry is an involutive reversing map. The next lemma asserts that the converse is also true. Note that a reversing map is not necessarily involutive. The following Jacobi diagram has a reversing map r satisfying $r^2 \neq 1$ and $r^4 = 1$:



under the AS and IHX relations. Also, note that $O(a, b, c, a, b, c) \in \mathcal{A}_{6,1}^{c,s}$ since one can find symmetry by flipping the half of the circle and by using the AS relation.

Remark 3.13. Suppose that n is odd. Since $\langle B_n^s \rangle = \text{tor } \mathcal{A}_{n,1}^c$ as shown in [15, Proposition 5.2], we see that $\langle B_n^s \rangle = \mathcal{A}_{n,1}^{c,s}$.

Let J (resp. \tilde{J}) be a connected Jacobi diagram of i-deg = n labeled by $\{1^\pm, \dots, g^\pm\}$ (resp. $\{1_j^\pm, \dots, g_j^\pm \mid j \in \mathbb{Z}_{\geq 1}\} \subset \mathcal{L}$ satisfying the condition in Definition 3.1). We call \tilde{J} a *lift* of J if \tilde{J} turns into J when we change the labels of \tilde{J} by ϖ . In this case, the Y_{n+2} -equivalence class $\tilde{\mathfrak{s}}(\tilde{J}) \in Y_n \mathcal{IC} / Y_{n+2}$ is a lift of $\mathfrak{s}(J) \in Y_n \mathcal{IC} / Y_{n+1}$. For a symmetric Jacobi diagram J with line symmetry $r: J \rightarrow J$, we also call \tilde{J} a *good lift* of J with respect to r if the difference between the subscripts of the labels $\ell(r(v))$ and $\ell(v)$ of \tilde{J} in \mathcal{L} is at most one for every univalent vertex $v \in U(J)$. It is obtained by choosing consecutive numbers as the subscripts of the labels in \mathcal{L} for each pair $(v, r(v))$ of univalent vertices such that $v \neq r(v)$.

Using the refined AS and refined STU relations, we obtain some elements in the kernels of $\mathfrak{s}: \mathcal{A}_n^c \rightarrow Y_n \mathcal{IC} / Y_{n+1}$ and $\tilde{\mathfrak{s}}: \mathbb{Z} \tilde{\mathcal{J}}_n^c \rightarrow Y_n \mathcal{IC} / Y_{n+2}$.

Theorem 3.14. *Let $n \geq 2$, and let J be a symmetric Jacobi diagram of i-deg = n labeled by $\{1^\pm, \dots, g^\pm\}$ with line symmetry $r: J \rightarrow J$. Let us denote by $\tilde{J} \in \mathbb{Z} \tilde{\mathcal{J}}_n^c$ a good lift of $J \in \mathcal{A}_n^c$ with respect to r , and denote $U^-(J) = \{v \in U(J) \mid \text{the subscript of } \ell(v) \text{ of } \tilde{J} \text{ is lower than that of } \ell(r(v))\}$.*

Then, we have the following.

(1) *When n is even,*

$$\sum_{\substack{v \in U(J) \\ r(v)=v}} \mathfrak{s}(\tilde{\delta}_v(\tilde{J})) + \sum_{v \in U^-(J)} \mathfrak{s}(\tilde{\delta}_{v r(v)}(\tilde{J})) = 0 \in Y_{n+1} \mathcal{IC} / Y_{n+2}.$$

(2) *When n is odd,*

$$2\tilde{\mathfrak{s}}(\tilde{J}) = - \sum_{v \in U(J)} \mathfrak{s}(\tilde{\delta}_v(\tilde{J})) - \sum_{v \in U^-(J)} \mathfrak{s}(\tilde{\delta}_{v r(v)}(\tilde{J})) \in Y_n \mathcal{IC} / Y_{n+2}.$$

Proof. The line symmetry $r: J \rightarrow J$ implies that the Jacobi diagram $\text{rev}(\tilde{J})$ is isomorphic to \tilde{J} if we map the labels of each Jacobi diagram by ϖ . Since \tilde{J} is a lift, all the labels of \tilde{J} and $\text{rev}(\tilde{J})$ are in $\{1_j^\pm, \dots, g_j^\pm \mid j \in \mathbb{Z}_{\geq 1}\}$ and $\{\bar{1}_j^\pm, \dots, \bar{g}_j^\pm \mid j \in \mathbb{Z}_{\geq 1}\}$, respectively. Change all the labels of univalent vertices in $\text{rev}(\tilde{J})$ as $a \mapsto \bar{a}$, and denote it by \tilde{J}_1 . By the refined AS relation among claspers and the AS relation, we have

$$\tilde{\mathfrak{s}}(\text{rev}(\tilde{J})) = (-1)^n \sum_{v \in U(J)} \mathfrak{s}(\tilde{\delta}_v(\tilde{J})) + (-1)^n \tilde{\mathfrak{s}}(\tilde{J}_1) \in Y_n \mathcal{IC} / Y_{n+2}. \quad (3.5)$$

The difference between \tilde{J}_1 and \tilde{J} is only the subscripts of the labels. Thus, if we exchange the subscripts of the labels of all $v \in U^-(J)$ in \tilde{J}_1 with that

Setting $J = O(a_1, a_2, \dots, a_m, \dots, a_3, a_2)$ in Theorem 3.14(1) and considering the line symmetry r which fixes the univalent vertices labeled by a_1 and a_m , we obtain the following. It is used in the proof of Theorem 1.1 in Section 5.

Corollary 3.17. *For $m \geq 2$ and $a_1, \dots, a_m \in \{1^\pm, \dots, g^\pm\}$,*

$$\begin{aligned} & O(a_1, \dots, a_{m-1}, a_m, a_{m-1}, \dots, a_1) + O(a_m, \dots, a_2, a_1, a_2, \dots, a_m) \\ & + \sum_{i=2}^{m-1} \theta(a_{i-1}, \dots, a_1, \dots, a_{i-1}; a_i; a_{i+1}, \dots, a_m, \dots, a_{i+1}) \in \text{Ker } \mathfrak{s}. \end{aligned}$$

Remark 3.18. By Corollary 3.17, we have $O(a_1, a_2, a_1) + O(a_2, a_1, a_2) \in \text{Ker } \mathfrak{s}$, which is proved in [15, Lemma 6.6(1)] in a different way. Now it is natural to ask whether

$$O(a_1, \dots, a_{m-1}, a_m, a_{m-1}, \dots, a_1) + O(a_m, \dots, a_2, a_1, a_2, \dots, a_m) \in \text{Ker } \mathfrak{s}$$

for $m \geq 3$. We see that the case $m = 3$ is true by Corollary 3.17 and Lemma 3.19 below.

Lemma 3.19. $\theta(a; b; c) = 0 \in \mathcal{A}_{5,2}^c$.

Proof. By the IHX relation, we have $\theta(a; c, b) = \theta(a; b; c) + \theta(a, b; c)$, where we use the notation (3.7) in the case $q = 0$. Here well-definedness of the map \mathbf{bu} defined in Section 4 implies that $\theta(a; c, b) = \mathbf{bu}(O(a, b, c)) = \theta(a, b; c)$, and hence $\theta(a; b; c) = 0$. \square

The Jacobi diagrams $T(a_1, a_2, \dots, a_{m+1}, \dots, a_2, a_1)$ and $O(a_1, a_2, \dots, a_m, \dots, a_2, a_1)$ are symmetric with respect to the apparent lines. The next corollary is obtained by applying Theorem 3.14(2) to these Jacobi diagrams.

Corollary 3.20. *Let $m \geq 2$ and $a_1, \dots, a_m \in \{1^\pm, \dots, g^\pm\}$. Let $J \in \mathbb{Z}\tilde{\mathcal{J}}_{2m-1}^c$ and $J' \in \mathbb{Z}\tilde{\mathcal{J}}_{2m-1}^c$ be good lifts respectively of the Jacobi diagrams $T(a_1, a_2, \dots, a_{m+1}, \dots, a_2, a_1)$ and $O(a_1, a_2, \dots, a_m, \dots, a_2, a_1)$ with respect to the line symmetries. Then, we have*

$$\begin{aligned} 2\tilde{\mathfrak{s}}(J) &= -\mathfrak{s}(T(a_1, a_2, \dots, a_{m+1}, a_{m+1}, \dots, a_2, a_1)) \\ &\quad - 2 \sum_{i=1}^m \mathfrak{s}(T(a_1, a_2, \dots, a_{i-1}, a_i, a_i, a_{i+1}, \dots, a_m, a_{m+1}, a_m, \dots, a_2, a_1)) \\ &\quad \pm \mathfrak{s}(O(a_{m+1}, a_m, a_{m-1}, \dots, a_2, a_1, a_2, \dots, a_{m-1}, a_m)) \\ &\quad + \sum_{i=2}^m \mathfrak{s}(\pm O(a_{m+1}, a_m, a_{m-1}, \dots, a_{i+1}, v_{i-1}, a_i, v_{i-1}, a_{i+1}, \dots, a_{m-1}, a_m)), \end{aligned}$$

$$\begin{aligned}
2\tilde{\mathfrak{s}}(J') &= -\mathfrak{s}(O(a_1, a_2, \dots, a_m, a_m, \dots, a_2, a_1)) \\
&\quad - 2 \sum_{i=1}^{m-1} \mathfrak{s}(O(a_1, a_2, \dots, a_{i-1}, a_i, a_i, a_{i+1}, \dots, a_m, \dots, a_2, a_1)) \\
&\quad + \sum_{i=1}^{m-1} \mathfrak{s}(\pm\theta(a_{i-1}, \dots, a_1, a_1, \dots, a_{i-1}; a_i; a_{i+1}, \dots, a_m, \dots, a_{i+1})) \in Y_{2m-1}\mathcal{IC}/Y_{2m+1}.
\end{aligned}$$

Here, $O(a_{m+1}, a_m, a_{m-1}, \dots, a_{i+1}, v_{i-1}, a_i, v_{i-1}, a_{i+1}, \dots, a_{m-1}, a_m)$ denotes the Jacobi diagram obtained by attaching $O(a_{m+1}, a_m, a_{m-1}, \dots, a_{i+1}, *, a_i, *, a_{i+1}, \dots, a_{m-1}, a_m)$ to two copies of $v_{i-1} = T(*, a_{i-1}, \dots, a_2, a_1)$ at the vertices labeled by $*$, and the signs \pm depend on the choice of a good lift.

Corollary 3.20 implies that most of the images of symmetric Jacobi diagrams of $i\text{-deg} = 2m - 1$ with 0-loop or 1-loop under \mathfrak{s} do not lift to torsion elements in $Y_{2m-1}\mathcal{IC}/Y_{2m+1}$. Moreover, in the case $m = 2$, we prove that the abelian group $Y_3\mathcal{IC}/Y_5$ is torsion-free.

In the following proof, we use Proposition 4.7: $\mathcal{A}_4^c \cong Y_4\mathcal{IC}/Y_5$ (to be shown later).

Proof of Theorem 1.2. Consider the exact sequence of abelian groups

$$0 \rightarrow Y_4\mathcal{IC}/Y_5 \rightarrow Y_3\mathcal{IC}/Y_5 \rightarrow Y_3\mathcal{IC}/Y_4 \rightarrow 0.$$

By [15, Theorem 1.7], we have $\text{tor}(Y_3\mathcal{IC}/Y_4) \cong (L_3 \oplus S^2(H)) \otimes \mathbb{Z}/2\mathbb{Z}$, where L_n denotes the degree n part of the free Lie algebra on H . Thus, the image of the set

$$X = \{T(a, b, c, b, a), T(b, c, a, c, b), T(a, b, b, b, a) \mid a \prec b \prec c\} \cup \{O(a', b', a') \mid a' \preceq b'\}$$

under the map \mathfrak{s} is a basis of $\text{tor}(Y_3\mathcal{IC}/Y_4)$ over $\mathbb{Z}/2\mathbb{Z}$, where \prec is a total order on the set $\{1^\pm, \dots, g^\pm\}$. For each $x \in X$, Example 3.16 (or Corollary 3.20) gives an element $x' \in \mathcal{A}_4^c$ satisfying $\mathfrak{s}(x') = 2\tilde{\mathfrak{s}}(\tilde{x}) \in Y_3\mathcal{IC}/Y_5$, where $\tilde{x} \in \tilde{\mathcal{J}}_3^c$ is a good lift of x . If the set $\{x' \mid x \in X\}$ extends to a basis of \mathcal{A}_4^c , then $Y_3\mathcal{IC}/Y_5$ is torsion-free. By focusing on 0-loop Jacobi diagrams with three pairs of identical labels in Corollary 3.20, it suffices to see that the set

$$\{T(a, b, c, c, b, a), T(b, c, a, a, c, b) \mid a \prec b \prec c\} \cup \{O(a, b, b, b), O(a', b', b', a') \mid a \prec b, a' \preceq b'\}$$

extends to a basis of $\mathcal{A}_4^c = \bigoplus_{l=0}^3 \mathcal{A}_{4,l}^c$. This is shown by Example 6.4 and [15, Proposition 5.2]. \square

Remark 3.21. Theorem 1.2 and the above exact sequence completely determine $Y_3\mathcal{IC}/Y_5$. Indeed, $Y_4\mathcal{IC}/Y_5$ and $(Y_3\mathcal{IC}/Y_4)/\text{tor}(Y_3\mathcal{IC}/Y_4)$ are computed in Proposition 4.7 and [15, Theorem 1.7].

Moreover, once $Y_5\mathcal{IC}/Y_6$ is determined, we accomplish the determination of the abelian group $Y_3\mathcal{IC}/Y_6$. To see it, we use the exact sequence

$$0 \rightarrow Y_5\mathcal{IC}/Y_6 \rightarrow Y_3\mathcal{IC}/Y_6 \rightarrow Y_3\mathcal{IC}/Y_5 \rightarrow 0.$$

Since this sequence splits by Theorem 1.2, one can determine $Y_3\mathcal{IC}/Y_6$. In particular, the inclusion induces an isomorphism $\mathrm{tor}(Y_5\mathcal{IC}/Y_6) \xrightarrow{\cong} \mathrm{tor}(Y_3\mathcal{IC}/Y_6)$.

We end this section by discussing the homology cobordism group \mathcal{IH} of homology cylinders (see [15, Section 2.1] for example). Recall that there is a natural projection $\mathcal{IC} \rightarrow \mathcal{IH}$, and let $Y_n\mathcal{IH}$ denote the image of $Y_n\mathcal{IC}$. Also, $[M], [N] \in \mathcal{IH}$ are said to be Y_n -equivalent if there is a sequence $M = M_1, M_2, \dots, M_r = N$ in \mathcal{IC} such that M_i and M_{i+1} are Y_n -equivalent or homology cobordant for $i = 1, 2, \dots, r-1$. Then we obtain an analogous sequence

$$0 \rightarrow Y_4\mathcal{IH}/Y_5 \rightarrow Y_3\mathcal{IH}/Y_5 \rightarrow Y_3\mathcal{IH}/Y_4 \rightarrow 0 \quad (3.8)$$

to the sequence in the proof of Theorem 1.2. However, this is not necessarily exact at the middle since the inclusion $Y_n\mathcal{IH} \subset \{[M] \in \mathcal{IH} \mid [M] \sim_{Y_n} [\Sigma_{g,1} \times [-1, 1]]\}$ might be proper.

Theorem 3.22. *The sequence (3.8) is exact and the module $Y_3\mathcal{IH}/Y_5$ is torsion-free.*

Proof. In [5, Corollary 51], it is shown that $\mathrm{Ker}(\mathfrak{s}: \mathcal{A}_{2n+1,0}^c \rightarrow Y_{2n+1}\mathcal{IH}/Y_{2n+2})$ coincides with $\mathrm{Im}(\Delta_{n,0}: \mathcal{A}_{n,0}^c \rightarrow \mathcal{A}_{2n+1,0}^c)$ when n is odd. Here the map $\Delta_{n,0}$ is defined in [15, Definition 3.4], which is denoted by Δ_{2n+1} in [4, Definition 4.3]. Also, $\mathfrak{s}: \mathcal{A}_{2n,0}^c \rightarrow Y_{2n}\mathcal{IH}/Y_{2n+1}$ is an isomorphism for all n ([5, Corollary 50]). Then, we have a commutative diagram

$$\begin{array}{ccccccc} 0 & \longrightarrow & \mathcal{A}_4^c & \xrightarrow{\mathfrak{s}} & Y_3\mathcal{IC}/Y_5 & \longrightarrow & Y_3\mathcal{IC}/Y_4 \longrightarrow 0 \\ & & \downarrow & & \downarrow & & \uparrow \mathfrak{s} \\ 0 & \longrightarrow & \mathcal{A}_{4,0}^c & \xrightarrow{\mathfrak{s}} & \frac{Y_3\mathcal{IC}/Y_5}{\mathfrak{s}(\mathcal{A}_{4,\geq 1}^c) + \mathfrak{s}(\mathbb{Z}\tilde{\mathcal{J}}_{3,\geq 1}^c)} & \dashrightarrow & \mathcal{A}_{3,0}^c / \mathrm{Im} \Delta_{1,0} \longrightarrow 0 \\ & & \cong \downarrow \mathfrak{s} & & \downarrow & & \cong \downarrow \mathfrak{s} \\ 0 & \longrightarrow & Y_4\mathcal{IH}/Y_5 & \longrightarrow & Y_3\mathcal{IH}/Y_5 & \longrightarrow & Y_3\mathcal{IH}/Y_4 \longrightarrow 0. \end{array}$$

Here the vertical dashed arrow is induced by [9, Theorem 2]. The top and middle rows are exact by Proposition 4.7 and diagram chasing, respectively. Then the bottom row is also exact.

Now, the latter half of the statement is proved almost in the same way as Theorem 1.2. \square

4. STRUCTURES OF MODULES OF JACOBI DIAGRAMS

4.1. Maps \mathfrak{b}_u and \mathfrak{b}_d between Jacobi diagrams. We introduce some maps between modules of Jacobi diagrams, which enable us to understand well the value of the invariant \bar{z}_{2m-1} for $\mathfrak{s}(O(a_1, \dots, a_m, \dots, a_1))$ in Section 5. Also, we prove Theorem 1.3 in this subsection.

Definition 4.1 ([2]). The map $\mathbf{bu}: \mathcal{A}_{n,l}^c \rightarrow \mathcal{A}_{n+2,l+1}^c$ is defined by blowing up a trivalent vertex, that is, by replacing a trivalent vertex of a Jacobi diagram with a loop as in Figure 2.

The map \mathbf{bu} is well-defined, namely independent of the choice of a trivalent vertex. Indeed, since $J \in \mathcal{A}_n^c$ is connected, it suffices to compare the results of blowing up at adjacent trivalent vertices. One can directly check it by the AS and IHX relations.

The map \mathbf{bu} is called the insertion of a triangle into a vertex in [2, Section 7.2.2] (only for trivalent graphs). Also, in [2, Remark 7.10], it is mentioned that the insertion of a bubble into an edge, which equals $2\mathbf{bu}$, is not necessarily injective.

Recall that \mathcal{J}_n^c denotes the set of connected Jacobi diagrams of i-deg = n . Let $\mathcal{J}_{n,2}^c$ be the subset of \mathcal{J}_n^c consisting of Jacobi diagrams whose first Betti numbers are two, and let \mathcal{R} be the submodule of the free \mathbb{Z} -module $\mathbb{Z}\mathcal{J}_{n,2}^c$ generated by the AS, IHX, and self-loop relators. Then $\mathcal{A}_{n,2}^c = \mathbb{Z}\mathcal{J}_{n,2}^c/\mathcal{R}$. Here note that we call an element of $\mathcal{J}_{n,2}^c$ a Jacobi diagram which is not yet an equivalence class. The *spine* of a Jacobi diagram J is defined to be the graph obtained by collapsing edges incident to univalent vertices until there is no univalent vertex. When $J \in \mathcal{J}_{n,2}^c$, its spine is either the theta graph or eyeglass graph. Let Θ_n be the subset consisting of $J \in \mathcal{J}_{n,2}^c$ whose spine is the theta graph, and let \mathcal{R}_Θ be the submodule of $\mathbb{Z}\Theta_n$ generated by the AS and IHX relators among diagrams in Θ_n .

Let us define a map $f: \mathbb{Z}\mathcal{J}_{n,2}^c/\mathcal{AS} \rightarrow \mathbb{Z}\Theta_n/\mathcal{R}_\Theta$. For $J \in \Theta_n$, we simply set $f(J) = J$. For $J \notin \Theta_n$, under the AS relation, we may assume J is of the form

$$\begin{array}{c} * & & t_1 & \dots & t_r & & * \\ \vdots & & \vdots & & \vdots & & \vdots \\ * & & \vdots & & \vdots & & * \end{array}, \quad (4.1)$$

where t_1, \dots, t_r and $*$'s are (rooted) trees. Note that $*$'s are not important to define f . In this case, $f(J)$ is defined by

$$f(J) = \sum \begin{array}{c} t_{a_1} & \dots & t_{a_p} \\ \vdots & & \vdots \\ * & & * \\ \vdots & & \vdots \\ * & & * \end{array} - \sum \begin{array}{c} t_{a_1} & \dots & t_{a_p} \\ \vdots & & \vdots \\ * & & * \\ \vdots & & \vdots \\ * & & * \end{array}, \quad (4.2)$$

where the sums are taken over all (p, q) -shuffles for $p, q \geq 0$ with $p + q = r$, that is, $a_1 < \dots < a_p$ and $b_1 < \dots < b_q$. Note that each summation has 2^r terms.

Proposition 4.2. f is well-defined and induces an isomorphism $\mathcal{A}_{n,2}^c \rightarrow \mathbb{Z}\Theta_n/\mathcal{R}_\Theta$, namely all relations among 2-loop Jacobi diagrams arise from the theta graph. Moreover, the inverse is the map induced by the inclusion $\mathbb{Z}\Theta_n \hookrightarrow \mathbb{Z}\mathcal{J}_{n,2}^c$.

Proof. Let $J \in \mathcal{J}_{n,2}^c$ be a Jacobi diagram of the form (4.1). By a 180 degree rotation and the AS relation, J has another expression \check{J} as (4.1), with sign $(-1)^r$. Thus, we have to check $f(J) = f((-1)^r \check{J})$. Applying a 180 degree rotation and the AS relation to each term of $f((-1)^r \check{J})$, we obtain

$$\sum \left[\begin{array}{c} t_{a_1} \dots t_{a_p} \\ \vdots \\ \text{---} \\ t_{b_1} \dots t_{b_q} \\ \vdots \\ \text{---} \end{array} \right] - \sum \left[\begin{array}{c} t_{a_1} \dots t_{a_p} \\ \vdots \\ \text{---} \\ t_{b_1} \dots t_{b_q} \\ \vdots \\ \text{---} \end{array} \right], \quad (4.3)$$

where the sums are again taken over all (p, q) -shuffles. Let us show that the first (resp. second) sum above is equal to the first (resp. second) sum in the definition of f . We discuss only the first sum, and the proof for the second sum is almost the same. In the following proof, it is convenient to regard the IHX relation as Kirchhoff's law. Now, by the IHX relation, we have

$$\left[\begin{array}{c} t_{a_1} \dots t_{a_p} \\ \vdots \\ \text{---} \\ t_{b_1} \dots t_{b_q} \\ \vdots \\ \text{---} \end{array} \right] = \sum \left[\begin{array}{c} t_{a'_1} \dots t_{a'_{p'}} \\ \vdots \\ \text{---} \\ t_{a'_1} \dots t_{a'_{p'}} \\ \vdots \\ \text{---} \\ t_{b'_{q'}} \dots t_{b'_{q''}} \\ \vdots \\ \text{---} \\ t_{b'_1} \dots t_{b'_{q''}} \\ \vdots \\ \text{---} \end{array} \right], \quad (4.4)$$

where the sum is taken over all (p', p'') -shuffles and (q', q'') -shuffles for $p' + p'' = p$ and $q' + q'' = q$. The terms with $p' = q' = 0$ appear in the definition of $f(J)$ as well. Therefore, one should check that the rest of the terms cancel with each other when we expand each term of the first sum in (4.3) as (4.4). To see it, let $m = \max\{a'_1, \dots, a'_{p'}, b'_1, \dots, b'_{q'}\}$ and focus on the tree t_m . Each Jacobi diagram J' in the summation pairs with another one which is identical with J' except that the edge labeled by t_m is attached on the opposite side of the vertical edge of the spine. Such pairs are canceled by the AS relation.

In the rest of the proof, we show that f preserves the IHX and self-loop relations. Any Jacobi diagram $J \in \mathcal{J}_{n,2}^c$ with self-loop is, under the AS relation, of the form (4.1) such that the left or right circle has a single trivalent vertex. Then $f(J) = 0$ by the definition and well-definedness of f . When the IHX relation is applied except the central edge of the eyeglass graph, it is obviously preserved by f . Therefore, what we should consider

The maps \mathbf{bu} and \mathbf{bd} play an important role to investigate $\mathcal{A}_{n,2}^c$ in Section 5. Here we give an easy application of Theorem 1.3, which is used in the proofs of Theorem 6.9 and Proposition 4.7.

Lemma 4.4. *The map $\mathbf{bu}: \mathcal{A}_{n,1}^c \rightarrow \mathcal{A}_{n+2,2}^c$ is an isomorphism when $n \leq 3$, and thus $\mathcal{A}_{4,2}^c \cong S^2(H)$ and $\mathcal{A}_{5,2}^c \cong \mathcal{A}_{1,0}^c$.*

Proof. When $n \leq 3$, we have $\langle \Theta_n^{\geq 1} \rangle = \{0\}$ by Lemma 3.19. Hence, Theorem 1.3 implies that $\mathbf{bu}: \mathcal{A}_{n,1}^c \rightarrow \mathcal{A}_{n+2,2}^c$ is an isomorphism. The latter half of the statement follows from [15, Proposition 5.1] for instance. \square

The rest of this subsection is devoted to giving an interesting observation related with the facts

$$\begin{aligned} \Delta_{n,0}(J) \in \text{Ker}(\mathcal{A}_{2n+1,0}^c \xrightarrow{\mathfrak{s}} Y_{2n+1}\mathcal{IC}/Y_{2n+2} \twoheadrightarrow Y_{2n+1}\mathcal{IH}/Y_{2n+2}), \\ \Delta_{n,0}(J) \in \text{Ker}(\mathcal{A}_{2n+1,0}^c \xrightarrow{\mathfrak{s}} Y_{2n+1}\mathcal{IC}/Y_{2n+2} \xrightarrow{\bar{\mathfrak{s}}_{2n+2}} \mathcal{A}_{2n+2}^c \otimes \mathbb{Q}/\mathbb{Z}) \end{aligned}$$

shown respectively in [5, Lemma 42] and [15, Proposition 3.5]. Recall that \mathcal{IH} denotes the homology cobordism group of homology cylinders.

Proposition 4.5. *Let $J \in \mathcal{A}_{n,0}^c$. Then $\Delta_{n,0}(J) \in \text{Ker}(\pi \circ \mathfrak{s}_{2n+3,1} \circ \mathbf{bu})$.*

Now, it is natural to ask whether $\Delta_{n,0}(J) \in \text{Ker}(\mathcal{A}_{2n+1,0}^c \rightarrow Y_{2n+1}\mathcal{IC}/Y_{2n+2})$. The case $n = 1$ is shown in [15, Lemma 6.6(2)]. To prove Proposition 4.5, we prepare the lemma below. Let $\eta: \mathcal{A}_{n,0}^c \rightarrow H \otimes L_{n+1}$ denote a homomorphism used in [15, Section 5.2] or [3, Section 1], and $\iota: H \otimes L_{n+1} \hookrightarrow H^{\otimes(n+2)}$ be the homomorphism induced by the natural embedding of the degree $n + 1$ part L_{n+1} of the free Lie algebra on H .

Lemma 4.6. *For $J \in \mathcal{A}_{n,0}^c$, the element $\iota \circ \eta(J)$ is contained in the submodule*

$$\langle a_0 \otimes a_1 \otimes \cdots \otimes a_{n+1} + (-1)^n a_{n+1} \otimes \cdots \otimes a_1 \otimes a_0 \mid a_i \in \{1^\pm, \dots, g^\pm\} \rangle.$$

Proof. In this proof, when $v \neq w \in U(J)$, we distinguish $\ell(v)$ and $\ell(w)$ even if $\ell(v) = \ell(w)$. Let us fix $v \neq w \in U(J)$ and compare terms of the form $\ell(v) \otimes \cdots \otimes \ell(w)$ and $\ell(w) \otimes \cdots \otimes \ell(v)$ in $\iota \circ \eta(J)$. By the AS relation, we may assume J is of the form

$$\ell(v) \begin{array}{c} t_1 \quad \cdots \quad t_r \\ \vdots \quad \vdots \quad \vdots \end{array} \ell(w) = (-1)^n \ell(w) \begin{array}{c} \bar{t}_r \quad \cdots \quad \bar{t}_1 \\ \vdots \quad \vdots \quad \vdots \end{array} \ell(v),$$

where t_i is a (rooted) tree and \bar{t}_i is its mirror image, that is, the tree obtained by reversing the cyclic orders of t_i , and the bar has a different meaning in Section 3. Therefore, for each term of the form $\ell(v) \otimes a_1 \otimes \cdots \otimes a_n \otimes \ell(w)$, there is a term of the form $(-1)^n \ell(w) \otimes a_n \otimes \cdots \otimes a_1 \otimes \ell(v)$. \square

Recall that $\mathcal{A}_{n,l}^{c,s}$ denote the submodule of $\mathcal{A}_{n,l}^c$ generated by symmetric Jacobi diagrams.

Proof of Proposition 4.5. Under the isomorphism $\langle B_{2n+3}^s \rangle \cong H^{\otimes(n+2)} \otimes \mathbb{Z}/2\mathbb{Z}$ ([15, Proposition 5.2]), we have $\mathbf{bu}(\Delta_{n,0}(J)) = \iota \circ \eta(J)$ since asymmetric Jacobi diagrams in $\mathbf{bu}(\Delta_{n,0}(J))$ are canceled each other. By Lemma 4.6, $\mathbf{bu}(\Delta_{n,0}(J))$ is written as a sum of elements of the form $O(a_1, \dots, a_{n+2}, \dots, a_1) + O(a_{n+2}, \dots, a_1, \dots, a_{n+2})$. By Corollary 3.17 and the definition of π in Section 1, we conclude that $\mathbf{bu}(\Delta_{n,0}(J)) \in \text{Ker}(\pi \circ \mathfrak{s}_{2n+3,1})$. \square

4.2. Goussarov-Habiro conjecture. In this subsection, we prove the Goussarov-Habiro conjecture for the Y_5 -equivalence as a corollary of Proposition 4.7. We write L'_n for the degree n part of the free quasi-Lie algebra on H . Let D_n (resp. D'_n) denotes the kernel of the bracket map $H \otimes L_{n+1} \rightarrow L_{n+2}$ (resp. $H \otimes L'_{n+1} \rightarrow L'_{n+2}$). By [3, Theorem 1.1], we have an isomorphism $\mathcal{A}_{n,0}^c \cong D'_n$, and it is torsion-free if n is even. Since the natural projection $L'_n \rightarrow L_n$ is an isomorphism over \mathbb{Q} , one conclude $\text{rank } D'_n = \text{rank } D_n$, which is computed by Witt's formula for $\text{rank } L_n$ (see [10, Theorem 5.11] for example).

Proposition 4.7. *The module \mathcal{A}_4^c is isomorphic to the direct sum of D'_4 , $\mathcal{A}_{4,1}^c$, $S^2(H)$, and \mathbb{Z} . In particular, \mathcal{A}_4^c is torsion-free, and thus $\mathfrak{s}: \mathcal{A}_4^c \rightarrow Y_4\mathcal{IC}/Y_5$ is an isomorphism.*

Proof. Let us investigate each direct summand of $\mathcal{A}_4^c = \bigoplus_{l=0}^3 \mathcal{A}_{4,l}^c$. First, $\mathcal{A}_{n,0}^c \cong D'_n$ by [3, Theorem 1.1]. The 1-loop part $\mathcal{A}_{4,1}^c$ is determined in [15, Proposition 5.2], which is torsion-free (and its rank is given in Remark 4.8). It follows from Lemma 4.4 that $\mathcal{A}_{4,2}^c \cong \mathcal{A}_{2,1}^c \cong S^2(H)$. Also, one can check that $\mathcal{A}_{4,3}^c \cong \mathbb{Z}$ (see [2, Table 7.1] in the case of rational coefficients).

We then conclude that \mathcal{A}_4^c is torsion-free. Here recall the facts that $\mathfrak{s}: \mathcal{A}_4^c \rightarrow Y_4\mathcal{IC}/Y_5$ is surjective and that it is an isomorphism over \mathbb{Q} . These imply that $\mathfrak{s}: \mathcal{A}_4^c \rightarrow Y_4\mathcal{IC}/Y_5$ is an isomorphism. \square

Remark 4.8. By [15, Proposition 5.2], the rank of $\mathcal{A}_{4,1}^c$ is computed as follows:

$$\frac{1}{2} \frac{1}{4} (\varphi(1)(2g)^4 + \varphi(2)(2g)^2 + \varphi(4)2g) + \frac{1}{4}(2g+1)(2g)^2 = 2g^4 + 2g^3 + \frac{3}{2}g^2 + \frac{1}{2}g,$$

where φ is Euler's totient function.

As mentioned in Section 1, the Goussarov-Habiro conjecture is a fundamental question about a relation between the Y_n -equivalence and finite type invariants of homology cylinders. For the definition of finite type invariant, we refer the reader to [7], [8], and [11, Section 2.3].

The degree 4 part of the Y -reduction of the LMO functor \tilde{Z} gives a map $\tilde{Z}_4^Y: \mathcal{IC} \rightarrow \mathcal{A}_4^Y \otimes \mathbb{Q}$, which is a finite type invariant of degree at most 4 ([1, Theorem 7.11]), where \mathcal{A}_n^Y is the submodule of \mathcal{A}_n generated by Jacobi diagrams without strut. Moreover, it induces a homomorphism $\tilde{Z}_4^Y: Y_4\mathcal{IC}/Y_5 \rightarrow \mathcal{A}_4^c \subset \mathcal{A}_4^Y \otimes \mathbb{Q}$ satisfying $\tilde{Z}_4^Y \circ \mathfrak{s}_4 = \text{id}_{\mathcal{A}_4^c}$ up to sign. The next corollary is proved in much the same way as [15, Proposition 6.12] and [11, Section 5.1].

Corollary 4.9. *For $M, M' \in \mathcal{IC}$, they are Y_5 -equivalent if and only if $f(M) = f(M')$ for every finite type invariant f of degree at most 4.*

Proof. If $M \sim_{Y_5} M'$, then they are not distinguished by finite type invariants of degree at most 4 (see [11, Lemma 2.3] for instance).

Conversely, suppose that $f(M) = f(M')$ for every finite type invariant f of degree at most 4. Then we see $M \sim_{Y_4} M'$ by [15, Proposition 6.12], and $\tilde{Z}_4^Y(M) = \tilde{Z}_4^Y(M') \in \mathcal{A}_4^Y \otimes \mathbb{Q}$. Since $Y_4\mathcal{IC}/Y_5$ is a group ([7, Theorem 3], [8, Section 8.5]), there is $N \in Y_4\mathcal{IC}$ such that $M \sim_{Y_5} N \circ M'$. Thus, we have $\tilde{Z}_0^Y(N) = \emptyset$ and $\tilde{Z}_i^Y(N) = 0$ for $i = 1, 2, 3$. Now, by the formula

$$\tilde{Z}_4^Y(M) = \sum_{i=0}^4 \tilde{Z}_i^Y(N) \star \tilde{Z}_{4-i}^Y(M')$$

(see [1, Corollary 8.3] for the details), we conclude $\tilde{Z}_4^Y(N) = 0 \in \mathcal{A}_4^Y \otimes \mathbb{Q}$. Since $\tilde{Z}_4^Y : Y_4\mathcal{IC}/Y_5 \xrightarrow{\cong} \mathcal{A}_4^c \hookrightarrow \mathcal{A}_4^Y \otimes \mathbb{Q}$ is injective by Proposition 4.7, $N = 0 \in Y_4\mathcal{IC}/Y_5$, and hence M is Y_5 -equivalent to M' . \square

5. KERNEL OF \mathfrak{s} RESTRICTED TO $\mathcal{A}_{n,1}^c$

The module structure of $\mathcal{A}_{n,1}^c$ is determined in [15, Proposition 5.2]. Recall that $\langle B_n^s \rangle$ is the submodule of $\mathcal{A}_{n,1}^c$ generated by the set B_n^s written after Remark 3.12. To obtain a more precise description of $\langle B_n^s \rangle$, we introduce a necklace with arrow, and complete the proof of Theorem 1.1. Here, a necklace consists of beads which are elements of the set $\{1^\pm, \dots, g^\pm\}$ and a necklace of length n is considered up to the action of the dihedral group \mathfrak{D}_{2n} .

Definition 5.1. A *necklace with arrow* is a pair of a symmetric necklace and an arrow which is an axis of symmetry. An arrow points to either a bead or the midpoint of adjacent beads. The set \vec{N}_{2m} of necklaces with arrow is separated into subsets \vec{N}'_{2m} and \vec{N}''_{2m} , where \vec{N}'_{2m} (resp. \vec{N}''_{2m}) denotes the set of necklaces with arrow pointing to a single bead (resp. the midpoint of adjacent beads) as illustrated on the left (resp. right) in Figure 3. The right one is denoted by $O(a_1, \dots, a_m \uparrow a_m, \dots, a_1)$.

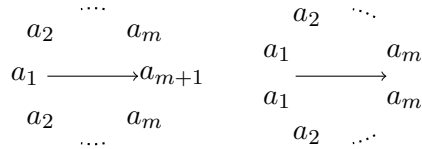


FIGURE 3. Two types of necklaces with arrow.

Note that considering a necklace with arrow is equivalent to fixing a base point on a necklace. The former is more convenient to discuss $\langle B_n^s \rangle$. Forgetting arrows, we obtain a natural map $\vec{N}_{2m} \twoheadrightarrow \langle B_{2m}^s \rangle$ (see Figure 4).

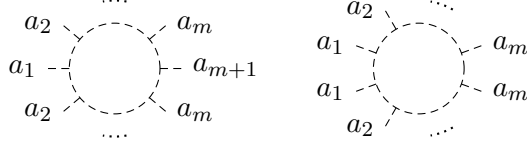


FIGURE 4. The Jacobi diagrams obtained from necklaces with arrow in Figure 3.

Also, we define a map $\mathfrak{mh}: \vec{N}_{2m}'' \rightarrow \langle B_{2m-1}^s \rangle$ by merging the two adjacent beads close to the head of the arrow, namely

$$\mathfrak{mh}(O(a_1, \dots, a_m \uparrow a_m, \dots, a_1)) = O(a_1, \dots, a_m, \dots, a_1).$$

Furthermore, this map induces an isomorphism $\mathfrak{mh}: (\mathbb{Z}/2\mathbb{Z})\vec{N}_{2m}'' \rightarrow \langle B_{2m-1}^s \rangle$ by [15, Proposition 5.2]. Similarly, $\mathfrak{mht}: \vec{N}_{2m}'' \rightarrow \langle B_{2m-2}^s \rangle$ is defined by merging the two beads close to the head and merging two beads close to the tail.

For each $x \in \vec{N}_{2m}$, there is a unique non-negative integer $e = e(x)$ such that $x = x^\pi = \dots = x^{\pi/2^{e-1}} \neq x^{\pi/2^e}$, where $x^{\pi/2^k}$ denotes the necklace with arrow obtained by rotating only the arrow of x by $\pi/2^k$.

Definition 5.2. Let $\iota: \vec{N}_{2m} \rightarrow \vec{N}_{2m}$ be the map defined by $\iota(x) = x^{\pi/2^e}$.

Example 5.3. For $a \neq b$, let $x = O(a, b, b, a, a, b, b, a \uparrow a, b, b, a, a, b, b, a) \in \vec{N}_{16}$. Then $e(x) = 2$, $\iota(x) = O(b, a, a, b, b, a, a, b \uparrow b, a, a, b, b, a, a, b)$, and

$$\begin{aligned} \mathfrak{mh}(x) &= O(a, b, b, a, a, b, b, a, b, b, a, a, b, b, a), \\ \mathfrak{mh}(\iota(x)) &= O(b, a, a, b, b, a, a, b, a, a, b, b, a, a, b) \in \mathcal{A}_{15,1}^{c,s}. \end{aligned}$$

Lemma 5.4. *The map ι is an involution without fixed point.*

Proof. The map ι is fixed point free by definition. Let $y = \iota(x)$ and $e = e(x)$. Then for $k = 0, 1, \dots, e-1$ we have $y^{\pi/2^k} = (x^{\pi/2^k})^{\pi/2^e} = x^{\pi/2^e} = y$. Also, $y^{\pi/2^e} = x^{\pi/2^{e-1}} = x$, and thus, $\iota(y) = x$. \square

Since $\#\vec{N}_{2m}' = (2g)^{m+1}$ and $\#\vec{N}_{2m}'' = (2g)^m$, Lemma 5.4 implies that $\#(\vec{N}_{2m}/\iota) = \frac{1}{2}((2g)^{m+1} + (2g)^m)$. It follows from the proof of [15, Proposition 5.2] that $\text{rank}_{\mathbb{Z}}\langle B_{2m}^s \rangle = \frac{1}{2}(2g+1)(2g)^m$. Therefore, a natural map $\mathbb{Z}\vec{N}_{2m} \twoheadrightarrow \langle B_{2m}^s \rangle$ induces an isomorphism $\mathbb{Z}(\vec{N}_{2m}/\iota) \rightarrow \langle B_{2m}^s \rangle$. This isomorphism enables us to identify connected symmetric Jacobi diagrams with necklaces with arrow.

We consider the composite map

$$\mathcal{A}_{2m-1,1}^c \xrightarrow{s} Y_{2m-1}\mathcal{IC}/Y_{2m} \xrightarrow{\bar{z}_{2m,2}} \mathcal{A}_{2m,2}^c \otimes \mathbb{Q}/\mathbb{Z}$$

Since the image of this homomorphism is included in $\mathcal{A}_{2m,2}^c \otimes (\frac{1}{2}\mathbb{Z}/\mathbb{Z})$, one obtains a homomorphism

$$\mathcal{A}_{2m-1,1}^c \xrightarrow{(\bar{z}_{2m,2} \circ \mathfrak{s}) \otimes 2} \mathcal{A}_{2m,2}^c \otimes \mathbb{Z}/2\mathbb{Z}.$$

Moreover, it induces a homomorphism

$$f: \mathcal{A}_{2m-1,1}^c \rightarrow (\mathcal{A}_{2m,2}^c / \langle \Theta_{2m}^{\geq 1} \rangle) \otimes \mathbb{Z}/2\mathbb{Z} \xrightarrow{\text{b}\partial} \mathcal{A}_{2m-2,1}^c \otimes \mathbb{Z}/2\mathbb{Z},$$

which sends $O(a_1, a_2, \dots, a_m, \dots, a_2, a_1)$ to $O(a_1, a_2, \dots, a_m, \dots, a_2)$ by [15, Theorem 1.1].

Let us prove Theorem 1.1: $\text{rank}_{\mathbb{Z}/2\mathbb{Z}} \text{Ker}(\pi \circ \mathfrak{s}_{2m-1,1}) = \frac{1}{2}((2g)^m - (2g)^{\lceil m/2 \rceil})$ for $m \geq 2$. Note that $\text{Ker}(\pi \circ \mathfrak{s}_{2m-1,1}) \subset \text{tor } \mathcal{A}_{2m-1,1}^c$.

Proof of Theorem 1.1. It follows from Corollary 3.17 that

$$\left\langle \mathfrak{mh}(x) + \mathfrak{mh}(\iota(x)) \in \langle B_{2m-1}^s \rangle \mid x \in \vec{N}_{2m}^{e=0} \right\rangle \subset \text{Ker}(\pi \circ \mathfrak{s}_{2m-1,1}),$$

where $\vec{N}_{2m}^{e=0} = \{x \in \vec{N}_{2m}'' \mid e(x) = 0\}$. We prove that this inclusion is actually an equality, and then the proof is complete since the rank of the $\mathbb{Z}/2\mathbb{Z}$ -module on the left is $\frac{1}{2}((2g)^m - (2g)^{\lceil m/2 \rceil})$.

Since $\bar{z}_{2m,1}$ factors through π , we obtain $\text{Ker}(\pi \circ \mathfrak{s}_{2m-1,1}) \subset \text{Ker}(\bar{z}_{2m,1} \circ \mathfrak{s}_{2m-1,1})$. It follows from [15, Theorem 1.1] that for $J = O(a_1, \dots, a_{m-1}, a_m, a_{m-1}, \dots, a_1)$ we have

$$\bar{z}_{2m,1} \circ \mathfrak{s}(J) = \delta'(J) = \frac{1}{2}O(a_1, \dots, a_{m-1}, a_m, a_m, a_{m-1}, \dots, a_1).$$

Therefore, one obtains a commutative diagram

$$\begin{array}{ccc} (\mathbb{Z}/2\mathbb{Z})\vec{N}_{2m}'' & \longrightarrow & (\mathbb{Z}/2\mathbb{Z})(\vec{N}_{2m}/\iota) \\ \mathfrak{mh} \downarrow & & \downarrow \\ \langle B_{2m-1}^s \rangle & \xrightarrow{\bar{z}_{2m,1} \circ \mathfrak{s}} & \langle B_{2m}^s \rangle \otimes \mathbb{Z}/2\mathbb{Z}, \end{array}$$

where the vertical arrows are the isomorphisms explained above. We now conclude that

$$\text{Ker}(\bar{z}_{2m,1} \circ \mathfrak{s}_{2m-1,1}) \subset \left\langle \mathfrak{mh}(x) + \mathfrak{mh}(\iota(x)) \mid x, \iota(x) \in \vec{N}_{2m}'' \right\rangle.$$

When m is odd, this completes the proof since $\vec{N}_{2m}^{e=0}$ coincides with $\{x \in \vec{N}_{2m}'' \mid \iota(x) \in \vec{N}_{2m}''\}$.

We next discuss the case m even. Since $(\bar{z}_{2m,2} \otimes 2) \circ \mathfrak{s}(x) = \delta'(x) \in \langle \Theta_{2m}^{\geq 1} \rangle$ for $x \in \langle \Theta_{2m-1}^{\geq 1,s} \rangle$, the above map f factors through $\pi \circ \mathfrak{s}_{2m-1,1}$ as follows:

$$\begin{array}{ccc}
\mathcal{A}_{2m-1,1}^c & \xrightarrow{f} & \mathcal{A}_{2m-2,1}^c \otimes \mathbb{Z}/2\mathbb{Z}, \\
\mathfrak{s}_{2m-1,1} \downarrow & & \uparrow \text{b\ddot{o}} \\
Y_{2m-1}\mathcal{IC}/Y_{2m} \xrightarrow{\bar{z}_{2m,2} \otimes 2} & (\mathcal{A}_{2m,2}^c / \langle \Theta_{2m}^{\geq 1} \rangle) \otimes \mathbb{Z}/2\mathbb{Z} & \\
\pi \downarrow & \nearrow & \\
(Y_{2m-1}\mathcal{IC}/Y_{2m})/\mathfrak{s}(\langle \Theta_{2m-1}^{\geq 1,s} \rangle) & &
\end{array}$$

where the module $\langle \Theta_{2m-1}^{\geq 1,s} \rangle$ is defined in Section 1. Hence we have $\text{Ker}(\pi \circ \mathfrak{s}_{2m-1,1}) \subset \text{Ker } f$. Now, it suffices to show that

$$\left\langle \mathfrak{mh}(x) + \mathfrak{mh}(\iota(x)) \mid x \in \vec{N}_{2m}^{e \geq 1} \right\rangle \cap \text{Ker } f = \{0\},$$

where $\vec{N}_{2m}^{e \geq 1} = \{x \in \vec{N}_{2m}'' \mid e(x) \geq 1, \iota(x) \in \vec{N}_{2m}''\}$. Note that any $x \in \vec{N}_{2m}^{e \geq 1}$ can be uniquely written as

$$x = O(\underbrace{w, \bar{w}, \dots, w, \bar{w}}_{2^e} \uparrow \underbrace{w, \bar{w}, \dots, w, \bar{w}}_{2^e})$$

for some word $w \in \{1^\pm, \dots, g^\pm\}^{m/2^e}$ with $w \neq \bar{w}$, where \bar{w} denotes the word obtained from w by reversing the order (see Example 5.5 below). By definition, we have

$$f(\mathfrak{mh}(x) + \mathfrak{mh}(\iota(x))) = \mathfrak{mht}(x) + \mathfrak{mht}(\iota(x)) \in \langle B_{2m-2}^s \rangle \otimes \mathbb{Z}/2\mathbb{Z}$$

for $x \in \vec{N}_{2m}^{e \geq 1}$. This element is contained in

$$\langle B_{2m-2}^{s,\text{period}} \rangle \otimes \mathbb{Z}/2\mathbb{Z} \cong \langle B_{m-1}^s \rangle \cong H^{\otimes m/2} \otimes \mathbb{Z}/2\mathbb{Z}.$$

See [15, Lemma 5.3] for the definitions of the superscript ‘‘period’’ and the first isomorphism, and here recall Remark 3.12. Under these isomorphisms, the image of $x = O(w, \bar{w}, \dots, w, \bar{w} \uparrow w, \bar{w}, \dots, w, \bar{w})$ is $w\bar{w} \cdots w\bar{w} + \bar{w}w \cdots \bar{w}w$, where each term consists of 2^{e-1} words. Since these two terms are linearly independent in $H^{\otimes m/2} \otimes \mathbb{Z}/2\mathbb{Z}$, this completes the proof. \square

Example 5.5. For $a \neq b$, let $x = O(a, b, b, a, a, b, b, a \uparrow a, b, b, a, a, b, b, a) \in \vec{N}_{16}$. Then $w = ab$, $\bar{w} = ba$, and x is sent to $abba + baab \in H^{\otimes 4} \otimes \mathbb{Z}/2\mathbb{Z}$.

6. KERNEL OF \mathfrak{s} RESTRICTED TO $\mathcal{A}_{n,l}^c$ FOR $l > 1$

We introduce a weight system, and prove Theorem 6.9 which gives lower bounds on the ranks of the $\mathbb{Z}/2\mathbb{Z}$ -modules $\text{Ker}(\mathfrak{s}|_{\text{tor } \mathcal{A}_{2k+1,k}^c})$ and $\text{Im}(\mathfrak{s}|_{\text{tor } \mathcal{A}_{2k+1,k}^c})$ for $k \geq 0$.

One usually constructs a weight system from a Lie algebra over \mathbb{C} (see [2, Section 6.3] for instance). However, we need to define it over \mathbb{Z} . Let R be a

commutative unital ring, and let \mathfrak{g} be a free R -module with a basis $\{e_i\}_{i=1}^d$. Suppose $c_{ijk} \in R$ ($i, j, k = 1, \dots, d$) satisfy that

$$c_{ijk} = -c_{jik}, \quad (6.1)$$

$$\sum_{m=1}^d (c_{ijm}c_{mkl} - c_{lim}c_{mjk} + c_{ljm}c_{mik}) = 0, \quad (6.2)$$

$$c_{iik} = 0, \quad (6.3)$$

$$c_{ijk} = c_{jki} = c_{kij}. \quad (6.4)$$

These conditions arise from a Lie algebra as follows. Let \mathfrak{g} be a Lie algebra over R with basis $\{e_i\}_{i=1}^d$. (While R is not a field but a ring, we use the terminology ‘‘Lie algebra’’.) Define the structure constants $c_{ijk} \in R$ by $[e_i, e_j] = \sum_k c_{ijk}e_k$ and suppose they satisfy $\delta([e_i, e_k], e_j) = \delta(e_i, [e_k, e_j])$ (see [2, Appendix A.1] for example). Here δ is the bilinear form defined by $\delta(e_i, e_j) = \delta_{ij}$, where δ_{ij} denotes the Kronecker delta. Then one can check that the c_{ijk} ’s satisfy the conditions (6.1)–(6.4).

Example 6.1. Let \mathfrak{g} be a semi-simple Lie algebra over \mathbb{C} . Then the structure constants c_{ijk} associated with an orthonormal basis with respect to the Killing form satisfy the conditions (6.1)–(6.4).

Let $H_R = H_1(\Sigma_{g,1}; R)$ and identify H_R with the R -module $R\{1^\pm, \dots, g^\pm\}$. For an R -module M , let $S(M)$ denote the symmetric algebra over R . Recall that $d = \text{rank}_R \mathfrak{g}$.

Definition 6.2. The *weight system* associated with \mathfrak{g} is a \mathbb{Z} -module homomorphism $W_{\mathfrak{g}}: \mathcal{A}_n \rightarrow S(H_R \otimes_R \mathfrak{g})$ defined as follows. Let $J \in \mathcal{A}_n$ be a Jacobi diagram, and let v_1, \dots, v_m (resp. w_1, \dots, w_n) be the univalent (resp. trivalent) vertices of J . Put labels $\{1, \dots, d\}$ on the edges of J , and let $c(w_l) = c_{ijk}$ if the edges adjacent to w_l are labeled by i, j, k in the cyclic order of w_l . Then, define $W_{\mathfrak{g}}(J) \in S^m(H_R \otimes_R \mathfrak{g})$ by

$$W_{\mathfrak{g}}(J) = \sum c(w_1) \cdots c(w_n) (l(v_1) \otimes e_{j_1}) \cdots (l(v_m) \otimes e_{j_m}),$$

where $j_i \in \{1, \dots, d\}$ is the label of the edge adjacent to v_i , and the sum is taken over all the ways of assigning labels to edges. Note that $c(w_l)$ depends only on the cyclic order by (6.4).

In other words, for a Jacobi diagram J without strut, we first put $t = \sum_{i,j,k} c_{ijk} e_i \otimes e_j \otimes e_k \in \mathfrak{g}^{\otimes 3}$ at each trivalent vertex. Note that t is invariant under cyclic permutation by (6.4). Next, using the bilinear form δ , we take the contraction of the form

$$\mathfrak{g}^{\otimes 3} \otimes \mathfrak{g}^{\otimes 3} \rightarrow \mathfrak{g}^{\otimes 4}, \quad (e_i \otimes e_j \otimes e_k, e_{i'} \otimes e_{j'} \otimes e_{k'}) \mapsto \delta(e_i, e_{i'}) e_j \otimes e_k \otimes e_{j'} \otimes e_{k'}$$

along every edge connecting two trivalent vertices (see [2, Section 6.2.1] for instance). Then, consider the tensor product $l(v_i) \otimes e_{j_i}$ at each univalent vertex v_i , and take the summation of the products of δ_{ij} ’s and $l(v_i) \otimes e_{j_i}$.

The weight system $W_{\mathfrak{g}}$ is well-defined since one can check that $W_{\mathfrak{g}}$ preserves the AS, IHX, and self-loop relations by (6.1), (6.2) and (6.3), respectively. For example, to prove that $W_{\mathfrak{g}}$ preserves (6.2), we consider

$$\begin{array}{ccc} \begin{array}{cc} i & j \\ \text{---} & \text{---} \\ | & | \\ \text{---} & \text{---} \\ l & k \end{array} & - & \begin{array}{cc} i & j \\ \text{---} & \text{---} \\ | & | \\ \text{---} & \text{---} \\ l & k \end{array} + \begin{array}{cc} i & j \\ \text{---} & \text{---} \\ \diagdown & \diagup \\ \text{---} & \text{---} \\ l & k \end{array}, \end{array}$$

where the central edge in each diagram is labeled by m which runs over $1, \dots, d$.

Example 6.3. Let $\mathfrak{g} = \langle e_1, e_2, e_3 \rangle_{\mathbb{Z}}$ and

$$c_{ijk} = \begin{cases} \text{sgn}(ijk) & \text{if } \#\{i, j, k\} = 3, \\ 0 & \text{if } \#\{i, j, k\} < 3. \end{cases}$$

One can directly check that these c_{ijk} 's satisfy (6.1)–(6.4). Also, it arises from $\mathfrak{sl}(2, \mathbb{C})$ with basis $\{(E + F)/2\sqrt{-1}, H/2\sqrt{-1}, (E - F)/2\}$, where

$$E = \begin{pmatrix} 0 & 1 \\ 0 & 0 \end{pmatrix}, \quad H = \begin{pmatrix} 1 & 0 \\ 0 & -1 \end{pmatrix}, \quad F = \begin{pmatrix} 0 & 0 \\ 1 & 0 \end{pmatrix}.$$

Here we give an example of computation. For $J = O(a, b) \in \mathcal{A}_{2,1}^c$, we have

$$W_{\mathfrak{g}}(O(a, b)) = -2(a \otimes e_1)(b \otimes e_1) - 2(a \otimes e_2)(b \otimes e_2) - 2(a \otimes e_3)(b \otimes e_3).$$

Note that the computation of this weight system corresponds to counting edge-colorings (with sign) by three colors $\{1, 2, 3\}$ such that all the three colors appear around each trivalent vertex.

Example 6.4. The weight system in Example 6.3 enables us show that the set $\{T(a, b, c, c, b, a), T(b, c, a, a, c, b)\}$ extends to a basis of $\mathcal{A}_{4,0}^c$ when $a, b, c \in \{1^{\pm}, \dots, g^{\pm}\}$ are mutually distinct. Indeed, one can check that the coefficients of $(a \otimes e_1)^2(b \otimes e_2)^2(c \otimes e_2)^2$ and $(a \otimes e_1)^2(b \otimes e_1)^2(c \otimes e_2)^2$ in $W_{\mathfrak{g}}(T(a, b, c, c, b, a)) \in S^6(H \otimes \mathfrak{g})$ are 1 and 0, respectively. On the other hand, the coefficients in $W_{\mathfrak{g}}(T(b, c, a, a, c, b))$ are 0 and 1, respectively.

In the rest of this section, we consider the weight system in Example 6.3, and simply write W . By Lemma 6.5 below, it induces a homomorphism

$$W_m: \mathcal{A}_n \otimes \mathbb{Q}/\mathbb{Z} \rightarrow S(H \otimes \mathbb{Z}e_m) \otimes \mathbb{Q}/\mathbb{Z}, \quad J \mapsto \frac{1}{2} \text{pr}_m \circ W(J),$$

where $\text{pr}_m: S(H \otimes \mathfrak{g}) \rightarrow S(H \otimes \mathbb{Z}e_m)$ denotes the projection.

Lemma 6.5. *Let $m \in \{1, 2, 3\}$ and $n \geq 1$. The image of the composite map $\mathcal{A}_n \xrightarrow{W} S(H \otimes \mathfrak{g}) \xrightarrow{\text{pr}_m} S(H \otimes \mathbb{Z}e_m)$ is included in $2S(H \otimes \mathbb{Z}e_m)$.*

Proof. We may assume $m = 1$, and use the comment at the end of Example 6.3. For each edge-coloring of a Jacobi diagram $J \in \mathcal{A}_n$ such that any edge adjacent to a univalent vertex is colored by 1, there is an edge-coloring

obtained by replacing all 2's (resp. 3's) with 3 (resp. 2). Therefore, the coefficient of $x \otimes e_1$ is even for $x \in H$. \square

We now give a useful relation between the weight system and the map \mathbf{bu} , which is essentially written, for example, in [2, Lemma 6.15 and Remark 6.16].

Lemma 6.6. $W(\mathbf{bu}^k(J)) = (-1)^k W(J)$ for any $k \geq 0$, where $\mathbf{bu}^k: \mathcal{A}_{n,l}^c \rightarrow \mathcal{A}_{n+2k,l+k}^c$ denotes the k times composition of \mathbf{bu} .

Proof. It suffices to prove the case $k = 1$. By the comment at the end of Example 6.3, for each edge-coloring of J , there is a unique edge-coloring of $\mathbf{bu}(J)$ extending it. This gives a bijection between the edge-colorings of J and those of $\mathbf{bu}(J)$, with opposite sign. This implies $W(\mathbf{bu}(J)) = -W(J)$. \square

Corollary 6.7 and Proposition 6.8 below are keys to prove Theorem 6.9.

Corollary 6.7. For any $a, b \in \{1^\pm, \dots, g^\pm\}$,

$$W_1 \circ \bar{z}_{2k+2,k+1} \circ \mathfrak{s} \circ \mathbf{bu}^k(T(a, b, a)) = \frac{1}{2}(a \otimes e_1)(b \otimes e_1) \in S(H \otimes \mathbb{Z}e_1) \otimes \mathbb{Q}/\mathbb{Z}.$$

In particular, $\bar{z}_{2k+2,k+1}$ is non-trivial.

Proof. Let $J = T(a, b, a)$. By [15, Theorem 1], we have

$$\bar{z}_{2k+2,k+1} \circ \mathfrak{s} \circ \mathbf{bu}^k(J) = \frac{1}{2} \delta''(\mathbf{bu}^k(J)) = \mathbf{bu}^k \left(\frac{1}{2} \delta''(J) \right).$$

It follows from Lemma 6.6 and $\delta''(J) = O(a, b)$ that $W_1 \circ \mathbf{bu}^k(\frac{1}{2} \delta''(J)) = W_1(\frac{1}{2} O(a, b))$. Finally, this is equal to $\frac{1}{2}(a \otimes e_1)(b \otimes e_1)$ by Example 6.3. \square

Proposition 6.8. $\mathfrak{s}(\mathbf{bu}^k(T(a, b, a))) = \mathfrak{s}(\mathbf{bu}^k(T(b, a, b))) \in Y_{2k+1} \mathcal{IC} / Y_{2k+2}$.

Proof. Let $J \in \mathbb{Z} \tilde{\mathcal{J}}_{2k,k}^c$ be a lift of $\mathbf{bu}^{k-1}(O(a, b))$. By Corollary 3.7, we have

$$\begin{aligned} \tilde{\mathfrak{s}}(J) &= \tilde{\mathfrak{s}}(\text{rev}(J)) \\ &= \tilde{\mathfrak{s}}(J) + \mathfrak{s}(\mathbf{bu}^{k-1}(O(a, b, a))) + \mathfrak{s}(\mathbf{bu}^{k-1}(O(b, a, b))). \end{aligned}$$

This completes the proof since $\mathbf{bu}^{k-1}(O(a, b, a)) = \mathbf{bu}^k(T(a, b, a))$. \square

In Appendix A, we give an alternative proof of Proposition 6.8 without using Corollary 3.7.

Theorem 6.9. For $g \geq 1$ and $k \geq 0$, the ranks of the $\mathbb{Z}/2\mathbb{Z}$ -modules $\text{Ker}(\mathfrak{s}|_{\text{tor } \mathcal{A}_{2k+1,k}^c})$ and $\text{Im}(\mathfrak{s}|_{\text{tor } \mathcal{A}_{2k+1,k}^c})$ are respectively greater than or equal to $g(2g-1)$ and $g(2g+1)$. Furthermore, the ranks are exactly $g(2g-1)$ and $g(2g+1)$ when $k = 0, 1, 2$.

Proof. In this proof, we write $\mathfrak{s}_{2k+1,k}$ for the restriction map $\mathfrak{s}|_{\text{tor } \mathcal{A}_{2k+1,k}^c}$. It follows from Proposition 6.8 that

$$\mathbf{bu}^k(T(a, b, a)) - \mathbf{bu}^k(T(b, a, b)) \in \text{Ker } \mathfrak{s}.$$

Here, by Corollary 6.7, one has $\mathbf{bu}^k(T(a, b, a)) \neq 0$. Comparing labels, we conclude that the above element is non-trivial and $\text{rank Ker } \mathfrak{s}_{2k+1,k} \geq \binom{2g}{2} = g(2g-1)$. Also, Corollary 6.7 implies that $\text{rank Im } \mathfrak{s}_{2k+1,k} \geq g(2g-1) + 2g = g(2g+1)$.

We finally show that the above inequality is an equality when $k = 0, 1, 2$. Since we have the exact sequence

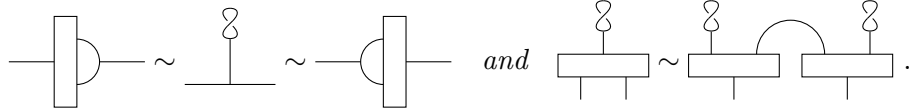
$$0 \rightarrow \text{Ker } \mathfrak{s}_{2k+1,k} \rightarrow \text{tor } \mathcal{A}_{2k+1,k}^c \rightarrow \text{Im } \mathfrak{s}_{2k+1,k} \rightarrow 0,$$

it suffices to see that $\text{rank tor } \mathcal{A}_{2k+1,k}^c \leq 4g^2$. By Lemma 4.4, the cases $k = 1, 2$ are reduced to the case $k = 0$. Then the proof is completed by the fact that $\text{tor } \mathcal{A}_{1,0}^c = \langle T(a, b, a) \mid a, b \in \{1^\pm, \dots, g^\pm\} \rangle$. \square

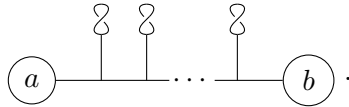
APPENDIX A. ALTERNATIVE PROOF OF PROPOSITION 6.8

In this appendix, we give an alternative proof of Proposition 6.8 by generalizing the proof of [15, Lemma 6.6(1)]. The key ingredients are twisted leaves and the zip construction. Every box in a clasper G has one output end and two input ends. To apply the zip construction to G , we need to specify a marking on G , which is a set of input ends of boxes. In the following proof, we do not specify markings but simply indicate which boxes are used. Here we review a useful lemma.

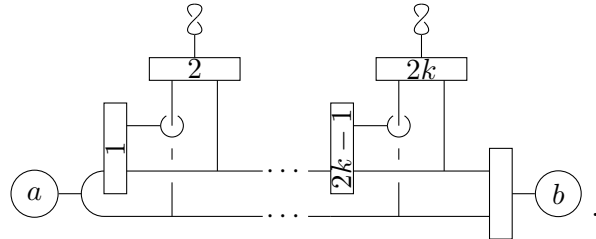
Lemma A.1 ([11, Lemma A.6]). *The following equivalences among claspers hold:*



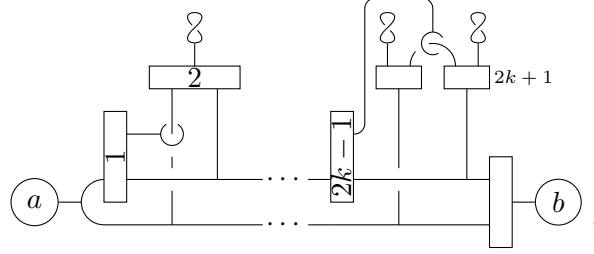
Proof of Proposition 6.8. Consider the clasper with $k+1$ twisted leaves (also called special leaves)



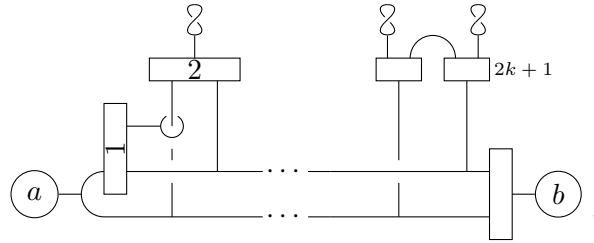
We first apply Lemma A.1 to the leftmost twisted leaf, and then a new box is created. Applying [8, Move 11] to this box k times from left to right, we obtain the equivalent clasper with $2k + 1$ boxes



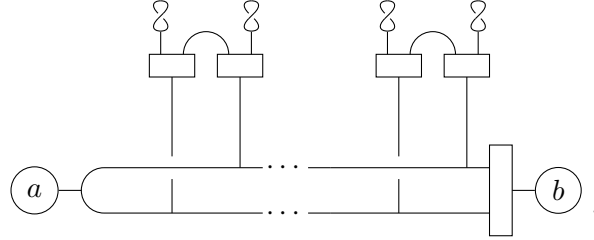
By Lemma A.1, this clasper is equivalent to



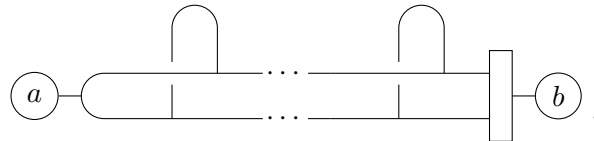
Apply the zip construction to the $k+1$ boxes with odd numbers so that one obtains a graph clasper G of degree $2k+1$ arising from the left-top input edge of Box $2k+1$ after using [8, Move 2]. Hence, by [11, Lemma A.1] (or [8, Moves 11 and 12]), G can be separated from the leaf connected to the right-top input edge of Box $2k-1$ up to Y_{2k+2} -equivalence. We next apply the same zip construction backward, and then we delete the leaf and Box $2k-1$ by [8, Move 3]:



In the same manner, one can delete Boxes $2k-3, \dots, 3$ and 1 in this order:



Here we choose one of the $2k$ boxes except the rightmost one, and apply [8, Move 11] to the box $2k+1$ times so that one obtains a graph clasper of degree $2k+1$ with a twisted leaf, which is deleted by [11, Lemma A.5] up to Y_{2k+2} -equivalence. Eventually, we obtain the clasper with a box



Here we use [8, Move 5 or 6], and get the right-hand side $\mathfrak{s}(\mathbf{bu}^k(T(b, a, b)))$ of the statement.

On the other hand, if we start the above procedure from the rightmost twisted leaf, then we get the left-hand side $\mathfrak{s}(\mathbf{bu}^k(T(a, b, a)))$. \square

REFERENCES

- [1] D. Cheptea, K. Habiro, and G. Massuyeau. A functorial LMO invariant for Lagrangian cobordisms. *Geom. Topol.*, 12(2):1091–1170, 2008.
- [2] S. Chmutov, S. Duzhin, and J. Mostovoy. *Introduction to Vassiliev knot invariants*. Cambridge University Press, Cambridge, 2012.
- [3] J. Conant, R. Schneiderman, and P. Teichner. Tree homology and a conjecture of Levine. *Geom. Topol.*, 16(1):555–600, 2012.
- [4] J. Conant, R. Schneiderman, and P. Teichner. Whitney tower concordance of classical links. *Geom. Topol.*, 16(3):1419–1479, 2012.
- [5] J. Conant, R. Schneiderman, and P. Teichner. Geometric filtrations of string links and homology cylinders. *Quantum Topol.*, 7(2):281–328, 2016.
- [6] S. Garoufalidis, M. Goussarov, and M. Polyak. Calculus of clovers and finite type invariants of 3-manifolds. *Geom. Topol.*, 5:75–108, 2001.
- [7] M. Goussarov. Finite type invariants and n -equivalence of 3-manifolds. *C. R. Acad. Sci. Paris Sér. I Math.*, 329(6):517–522, 1999.
- [8] K. Habiro. Claspers and finite type invariants of links. *Geom. Topol.*, 4:1–83, 2000.
- [9] J. Levine. Homology cylinders: an enlargement of the mapping class group. *Algebr. Geom. Topol.*, 1:243–270, 2001.
- [10] W. Magnus, A. Karrass, and D. Solitar. *Combinatorial group theory*. Dover Publications, Inc., Mineola, NY, second edition, 2004. Presentations of groups in terms of generators and relations.
- [11] G. Massuyeau and J.-B. Meilhan. Equivalence relations for homology cylinders and the core of the Casson invariant. *Trans. Amer. Math. Soc.*, 365(10):5431–5502, 2013.
- [12] J.-B. Meilhan. On surgery along Brunnian links in 3-manifolds. *Algebr. Geom. Topol.*, 6:2417–2453, 2006.
- [13] J.-B. Meilhan and A. Yasuhara. Milnor invariants and the HOMFLYPT polynomial. *Geom. Topol.*, 16(2):889–917, 2012.
- [14] S. Morita, T. Sakasai, and M. Suzuki. Torelli group, Johnson kernel, and invariants of homology spheres. *Quantum Topol.*, 11(2):379–410, 2020.
- [15] Y. Nozaki, M. Sato, and M. Suzuki. Abelian quotients of the Y -filtration on the homology cylinders via the LMO functor. *to appear in Geom. Topol.*
- [16] T. Ohtsuki. *Quantum invariants*, volume 29 of *Series on Knots and Everything*. World Scientific Publishing Co., Inc., River Edge, NJ, 2002. A study of knots, 3-manifolds, and their sets.

GRADUATE SCHOOL OF ADVANCED SCIENCE AND ENGINEERING, HIROSHIMA UNIVERSITY, 1-3-1 KAGAMIYAMA, HIGASHI-HIROSHIMA CITY, HIROSHIMA, 739-8526, JAPAN
Email address: nozakiy@hiroshima-u.ac.jp

DEPARTMENT OF MATHEMATICS, TOKYO DENKI UNIVERSITY, 5 SENJUSAHI-CHO, ADACHI-KU, TOKYO 120-8551, JAPAN
Email address: msato@mail.dendai.ac.jp

DEPARTMENT OF FRONTIER MEDIA SCIENCE, MEIJI UNIVERSITY, 4-21-1 NAKANO, NAKANO-KU, TOKYO, 164-8525, JAPAN
Email address: macksuzuki@meiji.ac.jp